Electrostatic and electrokinetic contributions to the elastic moduli of a driven membrane

D. Lacoste[1], G. I. Menon[2], M. Z. Bazant[1,3], and J. F. Joanny[4]

[1] Laboratoire de Physico-Chimie Théorique, UMR 7083, ESPCI, 10 rue Vauquelin, 75231 Paris Cedex 05, France
[2] The Institute of Mathematical Sciences, C.I.T Campus, Taramani, Chennai 600 113, India
[3] Department of Mathematics, Massachusetts Institute of Technology, Cambridge Massachusetts 02139, USA
[4] Institut Curie, UMR 168, 26 rue d'Ulm 75005 Paris, France

October 27, 2008

Abstract. We discuss the electrostatic contribution to the elastic moduli of a cell or artificial membrane placed in an electrolyte and driven by a DC electric field. The field drives ion currents across the membrane, through specific channels, pumps or natural pores. In steady state, charges accumulate in the Debye layers close to the membrane, modifying the membrane elastic moduli. We first study a model of a membrane of zero thickness, later generalizing this treatment to allow for a finite thickness and finite dielectric constant. Our results clarify and extend the results presented in [D. Lacoste, M. Cosentino Lagomarsino, and J. F. Joanny, Europhys. Lett., **77**, 18006 (2007)], by providing a physical explanation for a destabilizing term proportional to $k_\perp^3$ in the fluctuation spectrum, which we relate to a nonlinear (E^2) electro-kinetic effect called induced-charge electro-osmosis (ICEO). Recent studies of ICEO have focused on electrodes and polarizable particles, where an applied bulk field is perturbed by capacitive charging of the double layer and drives flow along the field axis toward surface protrusions; in contrast, we predict "reverse" ICEO flows around driven membranes, due to curvature-induced tangential fields within a non-equilibrium double layer, which hydrodynamically enhance protrusions. We also consider the effect of incorporating the dynamics of a spatially dependent concentration field for the ion channels.

PACS. 87.16.-b Subcellular structure and processes – 82.39.Wj Ion exchange, dialysis, osmosis, electro-osmosis, membrane processes – 05.70.Np Interface and surface thermodynamics

1 Introduction

Phospholipid molecules self-assemble into a variety of structures, including bilayer membranes, when placed in an aqueous environment[1]. The physical properties of such membranes, at thermal equilibrium, are controlled by a small number of parameters, including the surface tension and the curvature moduli. Understanding how these properties are modified when the membrane is driven out of equilibrium either by externally applied or internally generated electric fields, is a problem of considerable importance to the physics of living cells.

Applied electric fields can be used to drive shape changes in lipid membranes[2]. Artificial lipid vesicles can be produced, via a process called electroformation, by applying an AC electric field to a lipid film deposited on an electrode. Applying an electric field to a vesicle can also lead to the formation of pores via electroporation, a technique of relevance to gene or drug delivery. The role of the field in this case is to introduce transient pores, temporarily removing the barrier presented by the cell membrane to transmembrane transport.

Large electric fields are also generated internally in living cells. The transmembrane potential *in vivo* results from the action of a large number of membrane-bound ion pumps and channels. Resting potentials, and their modulation through excitation, are crucial to many cell functions [3]. Changes in the transmembrane potential and in the ion charge distribution close to the membrane accompany shape changes of cell membranes, such as those which occur when a cell divides. They also provide a means of communication between cells, as in the classic example of the action potential of neural cells [4,5].

Many aspects of electroformation, electroporation, and of the collective behavior of ion channels are as yet poorly understood [2,6]. This is because most studies of electrostatic effects in biological membranes have examined fluctuations at and close to thermal equilibrium [7–9,11–15]. However, membranes bearing ion pumps or channels which are driven by ATP hydrolysis ("active membranes"), or exposed to electric fields which lead to transmembrane currents in steady state, cannot be described in terms of equilibrium physics, in the first case because a non-equilibrium chemical potential for ATP molecules must be maintained externally to produce such driving and in the

second because a net current cannot flow in any system constrained by detailed balance.

To proceed beyond an equilibrium description of the membrane, it is necessary to account for forces generated by inclusions such as ion channels, pumps, or artificial pores [16–18]. An example of such an active membrane was discussed in Refs. [19,20]. In the experimental work described in these papers, a giant unilamellar vesicle was rendered active through the inclusion of light-activated bacteriorhodopsin pumps. These pumps transfer protons unidirectionally across the membrane as a consequence of conformational changes, when excited by light of a specific wavelength. In Ref. [20], a hydrodynamic theory for the non-equilibrium fluctuations of the membrane induced by the activity of the pumps was also developed. This work has stimulated substantial theoretical interest in the general problem of a proper description of non-equilibrium effects associated with protein conformational changes [21–25].

A major limitation of existing active membrane models is that they do not describe electrostatic effects associated with ion transport in detail. These effects are now understood to be very significant in the biological context. A recent paper, authored by two of us [26], addressed this limitation by studying the fluctuations of a membrane containing inclusions such as ion channels or pumps. Our analysis was based on the use of electrokinetic equations [27–29] supplemented by a simple description of ion transport in ion channels.

This paper augments Ref. [26] by providing details of the calculations and results presented there. It also presents fresh insights into the physical content of some of these results, while incorporating several new features, as detailed below. Our theoretical description of charge fluctuations near the membrane is in the same spirit as earlier work which examined the stability of shape fluctuations of a charged membrane using linear analysis [30]. We provide a simple physical picture for understanding the electrostatically induced part of the surface tension, which corresponds to a term proportional to $k_\perp^2$ in the free energy of the membrane. We do this by relating the surface tension to an integral over components of the electrostatic (Maxwell) stresses acting on the membrane and the fluid in the non-equilibrium steady state.

We also propose a physical interpretation of the term proportional to $k_\perp^3$ in the effective free energy, obtained first in Ref. [26]. We show that such a term is related to a nonlinear electrokinetic effect called "induced-charge electro-osmosis" (ICEO) [29], first described in the Russian colloids literature [31] and now studied extensively in microfluidics, since the discovery of electro-osmotic flows over electrode arrays applying AC voltages [32,28]. Steady ICEO flows also occur in DC fields around polarizable metallic [33,34] or dielectric [35,36] surfaces, and broken symmetries generally lead to fluid pumping or motion of freely suspended polarizable objects [29,37]. These phenomena are very general and should also be present in the case of a fluctuating membrane containing ion pumps and channels.

We also analyze the relaxation of a concentration field describing a non-uniform, but slowly varying, distribution of pumps and channels. We include the dynamics of the concentration field of the channels as in previous studies of fluctuations of membranes containing active or passive inclusions[21,38]. We first study the case of a membrane of zero thickness. We then generalize the model to the case of a bilayer of finite thickness and a finite dielectric constant, but with a uniform distribution of pumps and channels. This model allows a discussion of capacitive effects.

The results we present confirm the importance of capacitive effects in determining electrostatic and electrokinetic contributions to the elastic moduli of driven membranes[26]. They can be compared to results obtained in a recent study of electrostatic contributions to the elastic moduli of an equilibrium membrane of finite thickness[39]. The study of Ref. [39], which ignores ion transport, predicts a dependance of the bending modulus and tension as a function of the salt concentration which we compare to the one obtained in this paper, in the limiting case where no ion transport occurs in our model.

Our study is limited to the linear response of the ion channels and pumps. Real channels have a non-linear response which is essential for action potentials. Our study thus excludes these effects as well as other effects such as electro-osmotic instabilities [40], which originate in the non-linear response of the ion channels.

The outline of this paper is the following. In Section 2, we study a membrane with zero thickness in the linear response regime. We perform a systematic expansion about a flat membrane with a uniform distribution of pumps. We then discuss the charge fluctuations in the Stokes limit. In Section 3, we analyze ICEO flows around the driven membrane, emphasizing the basic physics of this new nonlinear electrokinetic phenomenon. In Section 4, we discuss the extension of the model to the case where the distribution of pumps/channels is non-uniform. In Section 5 we account for the finite thickness of the membrane. Finally, in Section 6 we summarize the results of this paper and indicate possible directions for further research. Appendix A describes a mapping between a driven membrane of finite thickness and an equivalent zero thickness membrane with appropriately modified boundary conditions while Appendix B illustrates the solution of the Stokes equation for the case of the membrane with zero thickness.

2 Electrostatically driven membrane of zero thickness

We begin by deriving the equation of motion of a driven membrane in an electrolyte in the limit in which the membrane has vanishing thickness and zero dielectric constant. We work in a linear regime and consider only steady state solutions. The quasi-planar membrane is located in the plane $z = 0$. It is embedded in an electrolyte and carries channels for two species of monovalent ions. The membrane itself is neutral, *i.e.* it bears no fixed charge. There
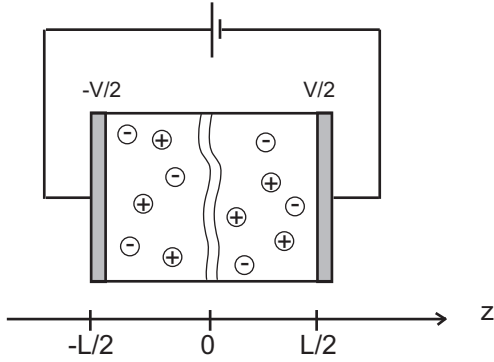
Fig. 1. Schematic of a quasi-planar membrane embedded in a symmetric electrolyte. The (bilayer) membrane is represented by the two wiggly lines near the plane $z = 0$. A voltage V is applied far from the membrane on electrodes separated by a distance L. Note that the electrode at potential $+V/2$ is called the anode and the one at $-V/2$ the cathode.

is an imposed potential difference V across the system of length L as shown in Figure 1.

The concentrations of the two ions are denoted by c_k, where the index k is 1 for the positive ion ($z_1 = 1$) and 2 for the negative ion ($z_2 = -1$). A point on the membrane is parameterized, in a Monge representation valid for small undulations, by a height function $h(\mathbf{r}_\perp)$, with $\mathbf{r}_\perp$ a two-dimensional vector.

The calculation proceeds via a perturbation theory about the planar or base state, to first order in the membrane height $h(\mathbf{r}_\perp)$, assuming a uniform concentration field for the channels/pumps. We denote dimensionful variables with a superscript $*$, dropping this superscript for variables which are made dimensionless. A summary of the dimensionful and dimensionless variables used in this paper and the correspondence between them is given in Table 1. To lighten the notation, the inverse Debye length κ, the diffusion coefficients for both species D_k, the electrolyte dielectric constant ϵ, the membrane dielectric constant in the finite thickness case ϵ_m, the charge of the electron e and the thermal energy $k_B T$, although dimensionful, will not carry a superscript $*$.

The potential obeys the Poisson equation

$$\nabla^{*2}\psi^* = -\left(\frac{ec_1^*}{\epsilon} - \frac{ec_2^*}{\epsilon}\right), \tag{1}$$

which becomes

$$\nabla^2\psi = -\left(\frac{c_1 - c_2}{2}\right), \tag{2}$$

when the following nondimensional variables are introduced: $c_k = c_k^*/n^*$, $\psi = e\psi^*/k_B T$, and $x = \kappa x^*$. Here

Unit	(1)	(2)	Relation
concentration	c_k^*	c_k	$c_k = c_k^*/n^*$
electrostatic potential	ψ^*	ψ	$\psi = e\psi^*/(k_B T)$
length	x^*	x	$x = \kappa x^*$
particle current	J_k^*	J_k	$J_k = J_k^*/(D_k n^* \kappa)$
chemical potential	μ^*	μ	$\mu = \mu^*/(k_B T)$
ionic current	i_k^*	i_k	$i_k = i_k^*/(D_k n^* \kappa)$
conductance	G_k^*	G_k	$G_k = G_k^* k_B T/(D_k n^* e^2 \kappa)$
charge density (at $z = 0^-$)	σ^*	σ	$\sigma = e\sigma^*/(\kappa\epsilon k_B T)$
pressure	p^*	p	$p = p^*/(2n^* k_B T)$
velocity	v^*	v	$v = v^*\eta^*\kappa/(2n^* k_B T)$

Table 1. Relation between dimensionful variables (column 1) generally denoted with the superscript $*$ and corresponding dimensionless variables (column 2). For notational simplicity, as discussed in the text, the inverse Debye length κ, the diffusion coefficients for both species D_k, the electrolyte dielectric constant ϵ, the membrane dielectric constant in the finite thickness case ϵ_m, the charge of the electron e and the thermal energy $k_B T$, although dimensionful, will not carry a superscript $*$.

n^* is the bulk concentration of the electrolyte at large distance from the membrane and κ is the inverse Debye-Hückel length with $\kappa^2 = 2e^2 n^*/\epsilon k_B T$.

We assume a symmetric distribution of ion concentrations on both sides of the membrane so that the Debye length is the same on both sides (the asymmetric distribution is discussed in Ref [26]).

We work with dimensionless currents, obtained by introducing $J_1 = J_1^*/(D_1 n^* \kappa)$ and $J_2 = J_2^*/(D_2 n^* \kappa)$, where D_1 and D_2 are the bulk diffusion coefficient of the positive and negative ions, and n^* is the bulk concentration of the electrolyte at large distance away from the membrane.

We use a Poisson-Nernst-Planck approach [3], in which ion currents are treated as constant. Assuming a steady state for ion concentrations, the equations of charge conservation take the form

$$\nabla \cdot (\nabla c_1 + c_1 \nabla \psi) = 0, \tag{3}$$
$$\nabla \cdot (\nabla c_2 - c_2 \nabla \psi) = 0. \tag{4}$$

The non-linear coupling between charge densities and potentials implies that general solutions of equations (2-4) are difficult to obtain analytically. However, as shown in Ref. [30], a solution can be obtained in terms of a series expansion. In this paper, we retain only the first term in such a series expansion. This is the Debye-Hückel approximation, and corresponds to linearizing equations (3-4). With the definitions $c_1 = 1 + \delta c_1$, $c_2 = 1 + \delta c_2$, we obtain

$$\nabla \cdot (\nabla\delta c_1 + \nabla\psi) = 0, \tag{5}$$
$$\nabla \cdot (\nabla\delta c_2 - \nabla\psi) = 0. \tag{6}$$

2.1 Base state charge distribution

The base state is defined with respect to the flat membrane, for which concentration and potential variations can only occur in the z direction. Denote by δN_1, δN_2

and Ψ, the base-state ion concentration profiles and the electrostatic potential, corresponding respectively to the variables δc_1, δc_2 and ψ of the previous section. Since the system is driven by the application of an electric field, this base state is a non-equilibrium steady state. There are constant particle currents for ions 1 and 2, denoted by J_1 and J_2, along the z direction. The equations of charge conservation in the bulk of the electrolyte are

$$\partial_z \delta N_1 + \partial_z \Psi = -J_1, \qquad (7)$$
$$\partial_z \delta N_2 - \partial_z \Psi = -J_2. \qquad (8)$$

To simplify notation, we introduce

$$Q = \frac{1}{2} \left(\delta N_1 - \delta N_2 \right). \qquad (9)$$

Thus, Q represents half the charge distribution. From equation (2), we have

$$\partial_z^2 \Psi + Q = 0. \qquad (10)$$

Equations (7-10) are to be solved with the following boundary conditions:

$$\delta N_1(z \to \pm L/2) = \delta N_2(z \to \pm L/2) = 0, \qquad (11)$$

$$\Psi(\pm L/2) = \pm V/2, \qquad (12)$$

far from the membrane. At the membrane surface, we enforce continuity of the electric field,

$$\partial_z \Psi_{z=0^+} = \partial_z \Psi_{z=0^-}, \qquad (13)$$

since we assume that the membrane has zero fixed charge.

There is, in general, a discontinuity in the potential, due to electrochemical equilibrium across the ion channels. This implies a distribution of surface dipoles on the membrane [41]. In the appendix, we derive a general Robin-type boundary condition for a thin dielectric membrane of thickness d

$$\delta_m \, \partial_z \Psi_{z=0^{\pm}} = \Psi(z = 0^+) - \Psi(z = 0^-) \qquad (14)$$

where

$$\delta_m = \frac{\epsilon \kappa d^*}{\epsilon_m}, \qquad (15)$$

which is also used to describe Stern layers and dielectric coatings on electrodes [42].

The limits of small thickness or small ϵ_m correspond to two distinct regimes with either $\delta_m \gg 1$ or $\delta_m \ll 1$. The regime $\delta_m \gg 1$, for equilibrium membranes, is called the decoupled limit in Ref. [7], because the electrical coupling between the layers is suppressed at large δ_m. This regime typically corresponds to the physical situation for biological membranes, since $\delta_m \gg 1$ implies that $\kappa d^* \gg 1/40$. Since the thickness of a typical lipid bilayer membrane is around 5nm, this translates to the requirement that the Debye length $\kappa^{-1} \ll 40d^* \simeq 200$nm, a condition which is usually satisfied. It is thus tempting to assume that we can take $\delta_m \to \infty$, thus reducing the Robin-type boundary condition to the form

$$\partial_z \Psi_{z=0^{\pm}} = 0. \qquad (16)$$

The boundary condition of Eq. (16), equivalent to the field vanishing at the surface of the membrane, is simple and convenient to work with for calculational purposes. However, the precise way in which the decoupled limit should be approached is, however, somewhat subtle in the non-equilibrium case.

As we show quantitatively in the appendix and discuss qualitatively further below, in a calculation in which the zero thickness case is derived explicitly as a limiting case of the finite thickness problem, the $\delta_m \to \infty$ limit corresponds to unrealistically large values of the ion channel conductance in comparison to the biological situation. This has specific implications for the sign of the diffuse charge at the membrane surface. In the first part of this paper, we will nevertheless assume $\partial_z \Psi_{z=0^{\pm}} = 0$ for the following reasons: The use of the simpler boundary condition of Eq. (16) leads to considerable calculational simplification as well as reproduces the profile of the electrostatic potential to reasonable accuracy. Thus, the physical underpinnings of many of our results, including the structure of ICEO flows, can be explained more easily in this limit. Our results in this limit may be more relevant to artificial membrane systems containing pumps and channels or their analogs in which conductances can be tuned to larger values than attainable *in vivo*. The biologically more relevant general case of finite-thickness membranes, for which no such simplifying approximation is made, is analyzed in the last part of the paper. The boundary condition (14) with finite δ_m is discussed in Appendix A.

With the assumptions above, in the limit $L \gg 1$, and for $z > 0$, we obtain

$$Q^+(z) = -\sigma e^{-z}, \qquad (17)$$
$$\Psi^+(z) = \sigma \left(z - \frac{L}{2} + e^{-z} \right) + \frac{V}{2}, \qquad (18)$$

and for $z < 0$,

$$Q^-(z) = \sigma e^{z}, \qquad (19)$$
$$\Psi^-(z) = \sigma \left(z + \frac{L}{2} - e^{z} \right) - \frac{V}{2}, \qquad (20)$$

where

$$\sigma = \frac{1}{2} \left(-J_1 + J_2 \right), \qquad (21)$$

is the normalized electrical current, and the superscripts $\pm$ refer to the regions of $z > 0$ and $z < 0$ respectively. The electric field component along z is $E_z^{\pm}(z) = -\partial_z \Psi^{\pm}$. For $z > 0$, we thus have

$$E_z^+(z) = \sigma \left(e^{-z} - 1 \right), \qquad (22)$$

and for $z < 0$

$$E_z^-(z) = \sigma \left(e^{z} - 1 \right). \qquad (23)$$

Note that in our dimensionless formulation $\mp \sigma = Q^+(0^{\pm}) - Q^-(0^{\pm})$ is also the normalized diffuse (ionic) charge density evaluated at the membrane surfaces, $z = 0^{\pm}$. The potential and the charge distribution calculated here are shown in Fig. 2.

In this model, the diffuse layers are intrinsically out of equilibrium and the non-zero DC current influences the distribution of ions through (21). Note that the sign of the non-equilibrium diffuse charge is negative on the positive side of the membrane *i.e.* $z = 0^+$, which we call the cathodic side (although it faces the anode) since positive charge flows towards it. We remind the reader that the cathode is the electrode located at $z = -L/2$ (see Figure 1), towards which positively charged cations drift, while negatively charged anions drift toward the anode at $z = L/2$.

This sign of the diffuse charge is unexpected – it is opposite to what is found in standard models for electrodes in a galvanic cell [42] or (potentiostatic) electrodialysis membranes [43] or in other related models of a membrane in an electric field [45], where diffuse charge resides in thin layers in Boltzmann equilibrium (up to the limiting current) and has the opposite sign, positive at the cathodic and negative at the anodic surfaces. Since biological membranes are typically much less conductive than the surrounding electrolyte, it is intuitively reasonable that positive charges should pile up under the action of the electric field directed from the anode to the cathode, near the positive side of the membrane. The "wrong" sign of the charge distribution obtained in Eqs. 17-20 and shown in Fig. 2 is thus an artefact of the approximation of zero thickness and zero dielectric constant. Physically, this unusual behavior may be attributed to the following: the positive charges which should pile up near the positive side are overcompensated by a charge of the opposite sign, in order to satisfy the boundary condition Eq. 16 of a zero electric field on the membrane.

Taking the limit of the general Robin-type boundary condition makes sense if $1/\delta_m$ vanishes. In reality, however, δ_m is finite and although it is larger than one, it is incorrect to assume an infinite δ_m in the calculation of the charge distribution. Using the more general boundary condition (14) with finite δ_m derived in the appendix A, and which is appropriate to describe a membrane of finite thickness and finite dielectric constant, we show in section 5 of this paper that *both signs of the charge distribution are possible in principle*. Under normal biological conditions, as we demonstrate using numerical estimates at the beginning of section 5.2, the membrane is much less conductive than the surrounding electrolyte and the diffuse charge distribution has the opposite sign as compared to that of Fig. 2.

We now discuss the boundary condition for the ion current at the membrane surface. This is ensured by choosing a specific relation between the current and the voltage at an ion pump or channel. In general such a relation is non-linear. We assume, for simplicity, a linear relation

$$J_k = -G_k \Delta\mu_k, \qquad (24)$$

where $\Delta\mu_k$ is the normalized chemical potential difference of ion k across the membrane, and G_k is a normalized conductance. This (dimensionless) conductance G_k is related
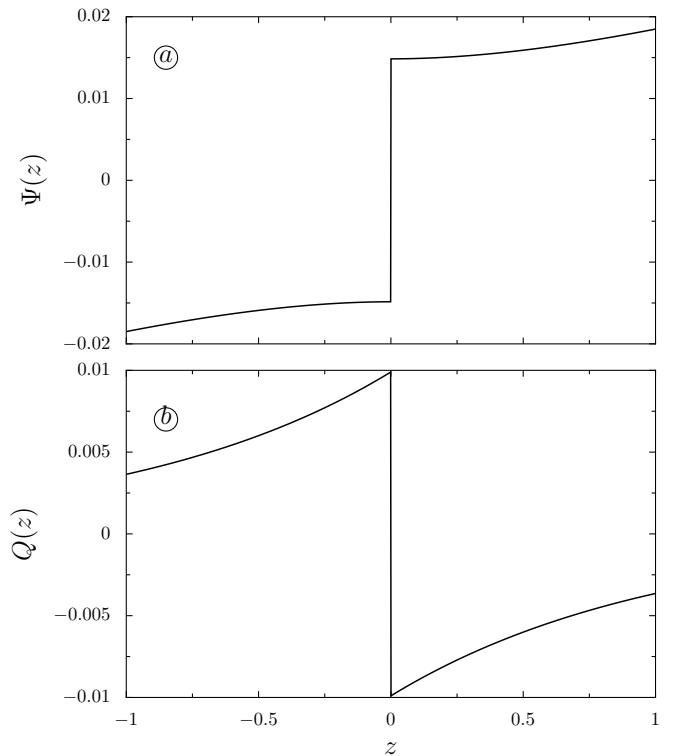

Fig. 2. Solutions of the electrokinetic equations for a membrane of zero thickness and symmetric ions concentrations. The electrostatic potential $\Psi(z)$ is shown in (a) and the quantity $Q(z)$ (which represents half the charge distribution) is shown in (b). We use dimensionless units and the following parameter values $V = 1$, $L = 100$, $G_1 = G_2 = 1$ and $k_\perp = 1$. In these conditions, $\sigma = 0.01$.

to the dimensionful conductance per unit area G_k^* by

$$G_k = \frac{G_k^* k_B T}{D_k^* n^* e^2 \kappa}, \qquad (25)$$

where the normalizing factor represents the conductance per unit area of a layer of electrolyte of thickness equal to $1/\kappa$ (one Debye layer). The normalized chemical potentials are defined by

$$\mu_1 = \delta N_1 + \Psi, \qquad (26)$$
$$\mu_2 = \delta N_2 - \Psi, \qquad (27)$$

and

$$\Delta\mu_k = \mu_k(z = 0^+) - \mu_k(z = 0^-). \qquad (28)$$

The currents are now determined self-consistently as

$$J_1 = -\frac{G_1 V}{1 + G_1 L}, \qquad (29)$$
$$J_2 = \frac{G_2 V}{1 + G_2 L}. \qquad (30)$$

Restoring dimensions, the electrical current is [26]

$$i_k^* = \frac{-G_k^* v_k^*}{1 + \frac{G_k^* L^* k_B T}{D_k n^* e^2}}, \qquad (31)$$

with $i_k^* = z_k e J_k^*$ the part of the total electric current associated with ion k of charge $z_k = \pm 1$, $v_k^* = V^* - V_{Nernst,k}^*$, and $V_{Nernst,k}^*$ the Nernst potential of ion k, which is zero here due to our assumption of symmetric concentrations. Note that σ^* has the units of charge per unit surface and is the surface charge of the Debye layers. It is related to σ defined in equation (21) by

$$\sigma^* = \frac{k_B T \kappa \epsilon \sigma}{e}. \tag{32}$$

The equivalent of equation (21) in dimensionful form is

$$\sigma^* = -\frac{1}{\kappa^2} \left(\frac{i_1^*}{D_1} + \frac{i_2^*}{D_2} \right). \tag{33}$$

This equation expresses the conservation of charge inside the Debye layers: for each ion k, the contribution in the surface charge of the Debye layer σ^*, is the product of the total electric current per unit area i_k^* carried by ion k, with the diffusion time $1/\kappa^2 D_k$ for the ion to diffuse over a length scale equal to the Debye length.

Equation (31) is consistent with the usual electric representation of ion channels in the ohmic regime in which the contribution of each ion taken in parallel. There are two conductances for each ion, accounting for the contributions of the electrolyte on both sides, and an electromotive force E_k in series[26]. The form of equations (17-20) is general and holds even when a non-linear current versus chemical potential relation is used in place of equations (24). However, our approach will be restricted to the linear regime for the ion channel response.

We stress that the form of this base state is general in the sense that the precise origin of the ion currents is immaterial because these currents are constant (independent of z). A qualitatively similar base state would describe the situation where such currents are created *internally* by active pumps, in the absence of any externally imposed potential difference or concentration gradients.

To complete the characterization of the base state, we calculate the stresses on the membrane. We define the stress tensor by

$$\tau_{ij}^* = \tau_{ij}^{H*} + \tau_{ij}^{M*}, \tag{34}$$

where τ_{ij}^{H*} and τ_{ij}^{M*} are the hydrodynamic and Maxwell stress tensors respectively, defined by

$$\tau_{ij}^{H*} = -P^* \delta_{ij} + \eta^* \left(\partial_i^* v_j^* + \partial_j^* v_i^* \right), \tag{35}$$

where η^* is the solvent viscosity and

$$\tau_{ij}^{M*} = \epsilon \left(E_i^* E_j^* - \delta_{ij} E^{*2}/2 \right). \tag{36}$$

In dimensionless form these are

$$\tau_{ij} = \tau_{ij}^H + \tau_{ij}^M, \tag{37}$$

with

$$\tau_{ij}^H = -P \delta_{ij} + \left(\partial_i v_j + \partial_j v_i \right), \tag{38}$$

and

$$\tau_{ij}^M = E_i E_j - \delta_{ij} E^2/2, \tag{39}$$

where E_i is the ith component of the electric field. The pressure P is the osmotic pressure of the ions in the Debye layers. In the base state, the condition $\nabla \cdot \tau = 0$ is equivalent to $\nabla P = Q E$, with Q and E given by equations (17-20).

With the boundary condition $P(z = \infty) = 0$, we obtain

$$P(z) = \sigma^2 \left(-e^{-z} + \frac{e^{-2z}}{2} \right), \tag{40}$$

for $z > 0$. Using equations (38-39), the stress on the positive side is calculated as $\tau_{zz}^+(z = 0) = \sigma^2/2$. It is straightforward to check that the same contribution exists on the negative side. Thus, overall, normal stresses are balanced in the base state, although a pressure gradient is present.

2.2 Interpretation of the electrostatic contribution to the surface tension

The extensive normal stresses discussed in the previous subsection can be argued to result in a positive electrostatic correction to the membrane surface tension (see Figure 3). This correction to the membrane tension Σ can be obtained from the knowledge of the electric field in the base state $E^{(0)}$ [26]. In our geometry, this correction can be written as

$$\Sigma = \int_{-\infty}^{\infty} [\tau_{xx}(z) - \tau_{zz}(z)] \, dz, \tag{41}$$

where τ_{xx} and τ_{zz} are components of the stress tensor. This derivation assumes incompressibility[44].

The electrostatic contribution to the surface tension is obtained from the Maxwell stress by $\Sigma = \Sigma_0 + \Sigma_1$ with :

$$\Sigma_0 = -\int_{-L/2}^{L/2} (E_z^{(0)})^2 (z) dz, \tag{42}$$

and

$$\Sigma_1 = \frac{L}{2} \left[(E_z^{(0)})^2 (z \to \infty) + (E_z^{(0)})^2 (z \to -\infty) \right]. \tag{43}$$

The term in Σ_1 ensures that the stress tensor remains divergence free. Both Σ_0 and Σ_1 contain contributions proportional to L, which originate from the pressure gradient in the fluid. As expected, these terms cancel each other in Σ. Substituting our previous expression for the electrostatic potential into equation (42), we find that $\Sigma = 3\sigma^2$. We will recover this result in the next section using a different method.

We now illustrate our physical picture for the origin of this electrostatic correction to the membrane tension. As shown in Figure 3, for a membrane of zero thickness, only Debye layers above and below the membrane contribute to the electrostatic correction to the membrane tension. The electrostatic force acting on the induced charges in the Debye layers on the positive and negative sides creates
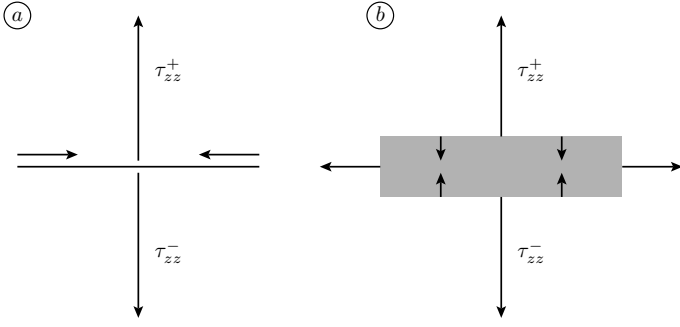
Fig. 3. Electrostatic corrections to the membrane tension for a membrane of zero thickness (a) and finite thickness (b). The Maxwell stresses are represented by vertical arrows while the horizontal arrows represent the resulting tension on the membrane as a consequence of incompressibility.

extensive stresses $\tau_{zz}^{\pm}$ near the membrane. These stresses, by incompressibility, tend to reduce the membrane area, thus producing an increase in the membrane tension. This can be termed as the "outside" contribution to the surface tension. In the case of a membrane of finite thickness there is, in addition to the "outside" contribution, an "inside" contribution. The "inside" contribution is in general dominant, because the largest voltage drop in this problem occurs across the membrane. This is a consequence of the large mismatch in dielectric constants between the membrane and the electrolyte ($\delta_m \gg 1$).

The "inside" contribution arises from compressive stresses (represented as opposing arrows within the shaded area on the figure on the right), which are generically present in any capacitor. These compressive stresses, directed along the z direction, produce lateral extensional stresses due to the conservation of the inside volume of the membrane. These stresses act to increase the membrane area, thus producing a negative electrostatic correction to the membrane tension. This contribution has been recognized to drive instabilities in membranes when a normal DC electric field is applied [6,39,45].

Recent experimental studies on the fluctuation spectrum of active membranes containing bacteriorhodopsin exhibit a lowering of the membrane tension in active vesicles as compared to passive ones [46]. This observation is consistent with the interpretation suggested above, where the lowering of the tension would be caused by a change in normal Maxwell stresses as a consequence of ion fluxes in or out of the vesicle. Although this interpretation appears plausible, alternate explanations are possible: further experimental work and theoretical modeling are necessary to confirm this proposal.

2.3 Charge fluctuations

In a linear approximation, the electrostatic potential can be written as a superposition of the base state contribution $\psi^{(0)}$ and a contribution linear in the membrane height field $\psi^{(1)}$. We work in the quasi-static approxima-

tion, which corresponds to angular frequency ω^* such that $\omega^* \ll D_k^* \kappa^2$. This approximation means that the membrane fluctuations occur on a time scale which is much slower than the time over which the electrostatic configuration adjust itself. Simple numerical estimates show that there is indeed such a separation of time scales [39]. This approximation allows us to solve the electrostatic problem for a fixed weakly curved geometry of the membrane.

With our previous notation: $q^{(0)} = Q$, $c_k^{(0)} = N_k$ and $\psi^{(0)} = \Psi$ in the base state, we now have

$$
\begin{aligned}
\psi(\mathbf{k}_\perp, z) &= \Psi(z) + \psi^{(1)}(\mathbf{k}_\perp, z), \\
q(\mathbf{k}_\perp, z) &= Q(z) + q^{(1)}(\mathbf{k}_\perp, z), \\
c_1(\mathbf{k}_\perp, z) &= N_1(z) + c_1^{(1)}(\mathbf{k}_\perp, z), \\
c_2(\mathbf{k}_\perp, z) &= N_2(z) + c_2^{(1)}(\mathbf{k}_\perp, z).
\end{aligned}
\tag{44}
$$

We use the following definition of Fourier transforms of an arbitrary function $g(\mathbf{r}_\perp, z)$

$$
g(\mathbf{k}_\perp, k_z) = \int d\mathbf{r}_\perp dz e^{-i(\mathbf{k}_\perp \cdot \mathbf{r}_\perp + k_z z)} g(\mathbf{r}_\perp, z),
\tag{45}
$$

and the inverse Fourier transform,

$$
g(\mathbf{r}_\perp, z) = \frac{1}{(2\pi)^3} \int d\mathbf{k}_\perp dk_z e^{i(\mathbf{k}_\perp \cdot \mathbf{r}_\perp + k_z z)} g(\mathbf{k}_\perp, k_z).
\tag{46}
$$

Consider now the contribution linear in the membrane height field $\psi^{(1)}$. The equations for the Fourier transforms of the charge distribution

$$
q^{(1)}(\mathbf{k}_\perp, z) = \frac{1}{2} \left(c_1^{(1)}(\mathbf{k}_\perp, z) - c_2^{(1)}(\mathbf{k}_\perp, z) \right)
\tag{47}
$$

and of the electrostatic potential $\psi(\mathbf{k}_\perp, z)$ follow from equations (2-6),

$$
\left(\partial_z^2 - k_\perp^2 \right) \psi^{(1)}(\mathbf{k}_\perp, z) + q^{(1)}(\mathbf{k}_\perp, z) = 0,
\tag{48}
$$

$$
\left(\partial_z^2 - k_\perp^2 \right) \left(q^{(1)}(\mathbf{k}_\perp, z) + \psi^{(1)}(\mathbf{k}_\perp, z) \right) = 0.
\tag{49}
$$

Since L is much larger than a Debye length, we can take the boundary conditions far from the membrane to be $\psi^{(1)}(\mathbf{k}_\perp, \pm\infty) = q^{(1)}(\mathbf{k}_\perp, \pm\infty) = 0$.

The relation between the current and the voltage at the membrane surface incorporating the contribution linear in the membrane height field is then calculated as

$$
\partial_z \left(c_1^{(1)}(\mathbf{k}_\perp, z) + \psi^{(1)}(\mathbf{k}_\perp, z) \right)_{z=h(\mathbf{r}_\perp)} = G_1 \times
$$
$$
\left(c_1^{(1)}(\mathbf{k}_\perp, 0^+) - c_1^{(1)}(\mathbf{k}_\perp, 0^-) + \psi^{(1)}(\mathbf{k}_\perp, 0^+) - \psi^{(1)}(\mathbf{k}_\perp, 0^-) \right),
$$
$$
\partial_z \left(c_2^{(1)}(\mathbf{k}_\perp, z) - \psi^{(1)}(\mathbf{k}_\perp, z) \right)_{z=h(\mathbf{r}_\perp)} = G_2 \times
$$
$$
\left(c_2^{(1)}(\mathbf{k}_\perp, 0^+) - c_2^{(1)}(\mathbf{k}_\perp, 0^-) - \psi^{(1)}(\mathbf{k}_\perp, 0^+) + \psi^{(1)}(\mathbf{k}_\perp, 0^-) \right),
\tag{50}
$$

These relations, the boundary conditions for the potential and the ion concentrations at infinity, as well as equation (48) are all satisfied when $c_1^{(1)}(\mathbf{k}_\perp, z) = -c_2^{(1)}(\mathbf{k}_\perp, z)$ and $q^{(1)}(\mathbf{k}_\perp, z) = -\psi^{(1)}(\mathbf{k}_\perp, z)$. This implies a zero flux

boundary condition for the contribution to first order in the membrane height field

$$\left(\partial_z q^{(1)} + \partial_z \psi^{(1)}\right)_{z=0} = 0. \tag{51}$$

At this order, whether the fluxes are directed along the normal $\hat{\mathbf{n}}$ rather than along $\hat{\mathbf{z}}$ is irrelevant, since the difference between $\hat{\mathbf{n}}$ and $\hat{\mathbf{z}}$ only introduces corrections to equation (51) which are of higher order than linear in h.

As a consequence, $\psi^{(1)}$ only depends on the zeroth order solution through the boundary conditions for the potential. The boundary condition for the total potential corresponds to a vanishing electric field at the membrane perturbed surface and is thus

$$\left(\partial_z \psi\right)_{z=h(\mathbf{r}_\perp)} = \left(h(\mathbf{r}_\perp)\partial_z^2 \Psi + \partial_z \psi^{(1)}\right)_{z=0} = 0. \tag{52}$$

Our final results for the potential thus are, for $z > 0$,

$$\psi^{(1)}(\mathbf{k}_\perp, z) = -q^{(1)}(\mathbf{k}_\perp, z) = \frac{h(\mathbf{k}_\perp)\sigma}{l} e^{-lz}, \tag{53}$$

and for $z < 0$,

$$\psi^{(1)}(\mathbf{k}_\perp, z) = -q^{(1)}(\mathbf{k}_\perp, z) = \frac{h(\mathbf{k}_\perp)\sigma}{l} e^{lz}, \tag{54}$$

where we have introduced

$$l = \sqrt{k_\perp^2 + 1}, \tag{55}$$

the characteristic inverse length of the electrostatic potential. The charge distribution and potential are even functions of z. Figure 2 exhibits the potential $\Psi(z)$ and $\psi^{(1)}(\mathbf{k}_\perp, z)$ in dimensionless units. This illustrates the discontinuity of the potential across the membrane, and the fact that the electric field vanishes at the membrane surface at zeroth order, as imposed by equation (16).

2.4 Membrane elasticity and force balance

In order to describe the coupling between the charge fluctuations in the electrolyte and the membrane, the Stokes equations must be solved with the appropriate boundary conditions, namely, the continuity of the velocity and the tangential stress constraints.

The elastic properties of the membrane are described by an Helfrich free energy

$$F_{mb} = \frac{1}{2} \int d^2\mathbf{r}_\perp [\kappa_0 \left(\nabla^2 h\right)^2 + \sigma_0 \left(\nabla h\right)^2], \tag{56}$$

where κ_0 is the bare bending modulus and σ_0 is the bare surface tension of the membrane.

The components of the stress tensor which act normal to the membrane are discontinuous, and that discontinuity is equal to the restoring force exerted by the membrane on the fluid, which is equal to

$$-\frac{\partial F_{mb}}{\partial h(\mathbf{r}_\perp)} = \sigma_0 \triangle h(\mathbf{r}_\perp) - \kappa_0 \nabla^4 h(\mathbf{r}_\perp). \tag{57}$$

2.5 Linear hydrodynamics of the membrane-fluid system

The equation of motion of the fluid, in the limit of low-Reynolds number and slow variation with time, is the Stokes equation supplemented by the condition of incompressibility. The governing equations, in dimensionless form, incorporating an arbitrary force density $\mathbf{f}$, are

$$\nabla \cdot \mathbf{v} = 0, \tag{58}$$
$$-\nabla p + \triangle \mathbf{v} + \mathbf{f} = 0. \tag{59}$$

We have rescaled the velocity by $2n^* k_B T/\eta^* \kappa$, and the pressure by $2n^* k_B T$. The Stokes equation (equation (59)) can be written equivalently as $\nabla \cdot \tau = 0$ in terms of the stress tensor of the fluid introduced in equations (38-39).

In view of the invariance of the problem with respect to translations parallel to the membrane surface, it is helpful to use the 2D Fourier representation introduced in Eqs. 45-46. As shown in Refs. [1,47], all vector fields in this problem can be decomposed into three components: longitudinal (*i.e.* along $\mathbf{k}_\perp$), transverse or normal (*i.e.* along $\hat{\mathbf{z}}$). These vectors form the triad $(\hat{\mathbf{k}}_\perp, \hat{\mathbf{n}}, \hat{\mathbf{t}})$, where $\hat{\mathbf{k}}_\perp = \mathbf{k}_\perp/k_\perp$, $\hat{\mathbf{n}} = \hat{\mathbf{z}}$ and $\hat{\mathbf{t}} = \hat{\mathbf{k}}_\perp \times \hat{\mathbf{n}}$. In such a coordinate system, the incompressibility condition takes the form

$$\partial_z v_z + i\mathbf{k}_\perp \cdot \mathbf{v}_\perp = 0, \tag{60}$$

and the Stokes equations become

$$-i\mathbf{k}_\perp p - k_\perp^2 \mathbf{v}_\perp + \mathbf{f}_\perp + \partial_z^2 \mathbf{v}_\perp = 0, \tag{61}$$
$$-\partial_z p + \partial_z^2 v_z - k_\perp^2 v_z + f_z = 0, \tag{62}$$
$$\partial_z^2 v_t - k_\perp^2 v_t + f_t = 0. \tag{63}$$

In the bulk of the electrolyte, we know the expression of the force $\mathbf{f}$. It is the electrostatic force acting on the local charge distribution, thus

$$\mathbf{f} = -q\nabla\psi, \tag{64}$$

which at first order in the perturbation defined in equation (44), is

$$\mathbf{f}_\perp(\mathbf{k}_\perp, z) = -i\mathbf{k}_\perp \psi^{(1)}(\mathbf{k}_\perp, z)Q(z),$$
$$f_z(\mathbf{k}_\perp, z) = -\nabla_z \psi^{(1)}(\mathbf{k}_\perp, z)Q(z)$$
$$- q^{(1)}(\mathbf{k}_\perp, z)\nabla_z \Psi(z). \tag{65}$$

Note that the force $\mathbf{f}$ above has no components along the transverse direction, and that the equation for v_t is decoupled from that of the other components of the velocity. In view of the boundary conditions appropriate here, we have $v_t = 0$ everywhere. Thus, we only need to consider the longitudinal and normal components. Although these components appear coupled in Eqs. 61-62, they can in fact be decoupled and the pressure can be eliminated. Indeed, the pressure can be obtained from Eq. 61. After using the incompressibility condition, the expression can be written in terms of only v_z and $\mathbf{f}_\perp$:

$$p = -\partial_z v_z + \frac{1}{ik_\perp}\mathbf{f}_\perp + \frac{1}{k_\perp^2}\partial_z^3 v_z. \tag{66}$$

After inserting this expression for the pressure in Eq. 61 and using the incompressibility condition of Eq. 60, one finds that the normal component of the velocity v_z obeys a single fourth order differential equation

$$\left(\partial_z^2 - k_\perp^2\right)\left(\partial_z^2 - k_\perp^2\right)v_z + \left(q^{(1)}\partial_z\Psi - \partial_z\psi^{(1)}Q\right) = 0. \quad (67)$$

The boundary conditions are: (i) continuity of the velocity, (ii) continuity of tangential constraints and (iii) discontinuity of the normal-normal component of the stress tensor. The equations of continuity for the velocity field are

$$v_z(z=0^+) = v_z(z=0^-) = \frac{\partial h(\mathbf{r}_\perp)}{\partial t}, \quad (68)$$

$$\mathbf{v}_\perp(z=0^+) = \mathbf{v}_\perp(z=0^-) = 0. \quad (69)$$

We have assumed, in writing equation (68), that there is a negligible amount of permeation of water across the bilayer, an assumption which should be suitable to describe most ion channels [20]. Although the membrane does permit the two-way flow of ions across it, the mechanical response of the membrane is dictated primarily by its relatively low permeability to water. Far from the membrane, we expect that

$$v_z(z\to\pm\infty) = p(z\to\pm\infty) = 0. \quad (70)$$

Interestingly, the boundary conditions for the transverse component of the velocity Eq. 69 together with the incompressibility condition Eq. 58 implies another continuity relation for the derivative of v_z [47]:

$$\left(\frac{\partial v_z}{\partial z}\right)_{z=0^+} = \left(\frac{\partial v_z}{\partial z}\right)_{z=0^-}. \quad (71)$$

The boundary conditions expressing the continuity of the tangential constraints (ii) and the discontinuity of the normal-normal component of the stress tensor (iii) are

$$-\tau_{\perp z}(z=0^+) + \tau_{\perp z}(z=0^-) = 0, \quad (72)$$

$$-\tau_{zz}(z=0^+) + \tau_{zz}(z=0^-) = -\frac{\partial F_{mb}}{\partial h(\mathbf{r}_\perp)}. \quad (73)$$

It is important to stress that this problem cannot be formulated only in terms of bulk forces, $i.e$ of the divergence of a stress tensor, because the hydrodynamic and Maxwell stress tensors enter the boundary conditions at the membrane surface explicitly. For this reason, the force of Eq. 64 only holds in the bulk, but the force localized on the membrane surface is unknown in this problem. It must be determined by enforcing the velocity and the stress boundary conditions.

2.6 Effective elastic moduli of the membrane

In this section, we give the equation of motion of the membrane which is obtained from the solution of the linear hydrodynamic equations. It is convenient to introduce

the growth rate s of the height fluctuation defined by $h(\mathbf{r}_\perp, t) = h(\mathbf{k}_\perp)\exp(i\mathbf{k}_\perp\cdot\mathbf{r}_\perp + st)$, so that the continuity equation for the normal component of the fluid velocity Eq. 68 can be written equivalently as

$$v_z(\mathbf{k}_\perp, z=0^\pm) = sh(\mathbf{k}_\perp). \quad (74)$$

As shown in Appendix B, the following equation of motion for the membrane results

$$s = -\frac{1}{4}\left(3\sigma^2 + \sigma_0\right)k_\perp + \sigma^2 k_\perp^2 - \left(\frac{3\sigma^2}{16} + \frac{\kappa_0}{4}\right)k_\perp^3. \quad (75)$$

In the particular case where $\sigma = 0$, corresponding to the case where there are no bulk electrostatic forces $\mathbf{f} = 0$, we recover a well-known relation [20], which can be written

$$s = -\frac{1}{4}\sigma_0 k_\perp - \frac{\kappa_0}{4}k_\perp^3, \quad (76)$$

or equivalently

$$\frac{\partial h(\mathbf{k}_\perp)}{\partial t} = -\frac{1}{4k_\perp}\frac{\partial F_{mb}}{\partial h(\mathbf{k}_\perp)}. \quad (77)$$

A convenient way to describe the effect of the additional terms arising in the equation of motion due to the electrostatic force when $\sigma \neq 0$ is to generalize Eq. 77 to

$$\frac{\partial h(\mathbf{k}_\perp)}{\partial t} = -\frac{1}{4k_\perp}\frac{\partial\left(F_{mb} + \delta F_{mb}\right)}{\partial h(\mathbf{k}_\perp)}, \quad (78)$$

where we have introduced an effective free energy δF_{mb} to account for the contribution of electrostatic stresses on the membrane. We stress that this definition does not imply that this effective free energy is to be understood in thermodynamic terms. It is merely a convenient way of understanding the role of each separate contribution to the stress tensor arising out of membrane fluctuations. Writing this effective free energy as

$$\delta F_{mb} = \frac{1}{2}\int d^2\mathbf{k}_\perp\, h(\mathbf{k}_\perp)h(-\mathbf{k}_\perp)[Kk_\perp^4 + \Sigma k_\perp^2 + \Gamma k_\perp^3], \quad (79)$$

we obtain electrostatic corrections to the elastic moduli of the membrane.

Since the second term in the right hand side of equation (75) is positive (a consequence of the fact that Γ is negative), a finite wavelength instability of a membrane or vesicle of low tension can occur when σ is sufficiently high [26]. We provide an estimate of the characteristic wavevector k_c below.

When non-thermal noise can be neglected, the fluctuation spectrum of the membrane height field can be obtained from equations (56-79),

$$\langle|h(\mathbf{k}_\perp)|^2\rangle = \frac{1}{(\sigma_0 + \Sigma)k_\perp^2 + \Gamma k_\perp^3 + (\kappa_0 + K)k_\perp^4}. \quad (80)$$

Such a spectrum is shown in Figure 9.

Our results are the following: We find an electrostatic correction to the surface tension $\Sigma = 3\sigma^2$, thus recovering the result obtained in equation (42). There is also

a positive correction to the bending modulus which is $K = 3\sigma^2/4$. Such terms are not surprising because they are present with the same sign in equilibrium charged membranes [7]. What is, however, surprising is the presence of a new purely non-equilibrium term in factor of $k_\perp^3$ in the free energy, $\Gamma = -4\sigma^2$. We propose a physical interpretation for this term in the sub-section which follows.

In dimensionful form, these moduli are $\Sigma^* = 3(\sigma^*)^2/\kappa$, $K^* = 3(\sigma^*)^2/4\kappa^3$ and $\Gamma^* = -4(\sigma^*)^2/\kappa^2$, in terms of σ^* the dimensionful surface charge, in agreement with Ref. [26]. For order-of-magnitude estimates, with $V^* = 50\text{mV}$, $L^* = 1\mu m$, $G_1^* = G_2^* = 10\Omega^{-1}/\text{m}^2$, $D_1 = D_2 = 10^{-5}\text{cm}^2/s$ and $n^* = 16.6\text{mM}$, we obtain $\Sigma^* = 3.2 \cdot 10^{-16}$ Jm^{-2}, $\Gamma^* = -10^{-24}$ Jm^{-1} and $K^* = 10^{-13} k_B T$. Although the ion flux is typical of ion channels, the moduli Σ^*, Γ^* and K^* are very small due to the strong dependance of these moduli on κ^{-1}, which is only 2.3nm here. As we show below, these low values also reflect the fact that we have, until now, neglected the bilayer character of the membrane and its finite capacitance.

The characteristic wavevector of the finite wavelength instability discussed in Eq. 75 is $k_c = -\Gamma/2(K + K_0)$ [26]. With the numerical estimates given above, and a typical value for the bare bending modulus of the membrane $K0$ of 10kT, one finds that k_c is of the order of 10^{-5}m^{-1}. This corresponds to a very large length scale, which indicates that this instability is unlikely to be observed in practice. A very different instability arises in a membrane of finite thickness when the tension becomes negative. That instability is a zero wavelength instability and is a real effect [6,39,45].

3 Electro-osmotic flow induced around the membrane

In this section, we propose an interpretation of the cubic term in $k_\perp$ with coefficient Γ in the effective free energy obtained above. Our arguments are based on the existence of nonlinear electro-osmotic flow around a curved membrane. This direct electrokinetic effect is present in addition to the usual viscous flow caused by membrane motion [48], shown in Figure 4(a), which couples indirectly to the electric field.

In our geometry, the electric field is directed mainly along the z direction. Our analysis of charge fluctuations indicated that perturbations in the membrane shape induced a tangential component of the electric field near the membrane. Such a tangential electric field acts on the diffuse charge in the diffuse layers, creating a effective hydrodynamic slip relative to the instantaneous membrane position. This electrokinetic effect creates an array of counter-rotating vortices around the membrane, illustrated in Figure 4(b), which tend to enhance shape perturbations.

The general phenomenon of nonlinear electro-osmotic flow around a polarizable surface has been termed "induced-charge electro-osmosis" (ICEO) [29]. It arises in a variety of situations involving polarizable surfaces, producing circulating flow patterns similar to those in our problem of
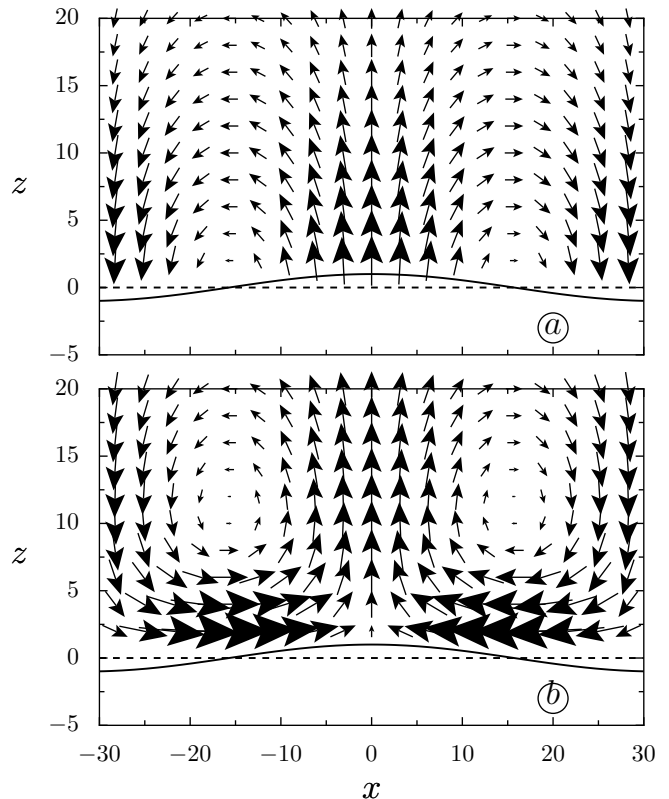

Fig. 4. Two types of fluid flow around a perturbed, driven membrane. (a) The membrane bending mode with associated flow field [48], in the absence of any applied electric field: $\sigma = 0$. In this case, it is the motion of the membrane which drives the flow field by the incompressibility condition. For a growing sinusoidal perturbation, streamlines connect the peaks to the valleys. The membrane seen edge-on as a solid line, undergoes a bending wave of wavevector 0.1 (or of wavelength 20π) and of amplitude 0.1. Note that the height of the membrane has been multiplied by an extra factor 10 for improved visualization. The undeformed membrane is shown edge-on as a dashed line. (b) Vortices of induced-charge electro-osmosis (ICEO) for a non-moving curved membrane, due to effective slip from the valleys to the peaks, as explained below. Unlike the case (a), here it is the flow field induced by ICEO which determines the modulation of this non-moving membrane. An applied field is applied which corresponds to $\sigma = 30$. In this example, as in biological membranes, the double layers are thin compared to the wavelength of the perturbation $k_\perp = k_\perp^*/\kappa \ll 1$. The calculation also assumes linear response to a small amplitude perturbation, $\kappa h^* \ll 1$. In these figures, this condition is satisfied since $h = 0.1$, and the unit length corresponds to one Debye length.

a fluctuating driven membrane. What we now call ICEO flow was first described by V. Murtsovkin and collaborators in Russia [31] in the case of metallic colloidal spheres. Recent interest in the subject has focused on novel phenomena in microfluidic devices, such as AC electro-osmotic flow around electrode arrays [32,28], ICEO flow around metal posts [33,34] and dielectric corners [35,36] and induced-charge electrophoresis [29,37]. However, we are not aware

of any prior theory or experiment describing ICEO around membranes.

The classical theory of electrokinetic phenomena assumes a constant surface charge, or equivalently, a constant voltage (zeta potential) between the shear plane at the surface and the quasi-neutral bulk electrolyte just outside the diffuse charge layer [27]. In that case, the presence of a tangential component of the electric field (approximately constant across the thickness of the double layer) leads to electro-osmotic flow that is linear in the field. For thin double layers, the effective hydrodynamic slip outside the double layer is given by the Helmholtz-Smoluchowski formula [27]

$$\mathbf{v}_\perp{}^* = -\frac{\epsilon \zeta^*}{\eta^*} \mathbf{E}_\perp{}^*, \qquad (81)$$

where ζ^* denotes the zeta potential across the diffuse part. This result holds in the asymptotic limit of thin double layers. It is also valid even if a normal current drives the diffuse charge out of equilibrium – all that is required is for the viscosity and permittivity to be constant within the double layer and for the bulk salt concentration to be uniform (without tangential gradients) [29,43]. At a polarizable surface, the zeta potential and tangential field component vary in response to perturbations of the system. This results in nonlinear ICEO flows which typically vary with the square of the applied voltage.

To understand the appearance of ICEO flow in our system, we begin by considering dominant balances in the dimensionless equations. We first consider the limit of thin double layers compared to the perturbation wavelength, $k_\perp \ll 1$ (or $k_\perp^* \ll \kappa$), which is relevant for biological membranes. In our system of normalized units, the electro-osmotic slip formula (81) predicts the scaling

$$\mathbf{v}_\perp(\mathbf{k}_\perp, z \geq 1) \simeq -\zeta \mathbf{E}_\perp(\mathbf{k}_\perp, z \to 0^+), \qquad (82)$$

where the effective slip velocity outside the double layer ($z \geq 1$) is proportional to the typical tangential electric field in the diffuse layer, set by its typical value within the Debye layer at the surface ($z \to 0^+$). Although the scaling is the same, a subtle difference with Helmholtz-Smoluchowski theory is that the tangential electric field is confined to the diffuse layer and vanishes in the neutral bulk electrolyte ($z \geq 1$).

The expression (82) can be verified by direct integration of the Stokes equation as follows. After projecting Eq. 59 in the transverse direction, and retaining only terms of first order, one obtains

$$\triangle \mathbf{v}_\perp + Q(z)\mathbf{E}_\perp{}^{(1)} = 0, \qquad (83)$$

which can be simplified using the condition $k_\perp \ll 1$ to give

$$\partial_z^2 \mathbf{v}_\perp(\mathbf{k}_\perp, z) + Q(z)\mathbf{E}_\perp{}^{(1)}(\mathbf{k}_\perp, z) = 0. \qquad (84)$$

Now from (53) in the limit $k_\perp \ll 1$,

$$\mathbf{E}_\perp{}^{(1)}(\mathbf{k}_\perp, z) = -i\mathbf{k}_\perp \psi^{(1)}(\mathbf{k}_\perp, z) = -i\mathbf{k}_\perp \sigma h(\mathbf{k}_\perp)e^{-z}. \qquad (85)$$

After inserting Eq 85 into Eq. 84, using the no-slip condition $\mathbf{v}_\perp{}^{(1)}(\mathbf{k}_\perp, z = 0^+) = 0$, the transverse first-order velocity profile is found to scale as (dropping a numerical prefactor of $i/4$)

$$\mathbf{v}_\perp{}^{(1)}(\mathbf{k}_\perp, z) \simeq \sigma^2 \mathbf{k}_\perp h(\mathbf{k}_\perp)(1 - e^{-2z}), \qquad (86)$$

a scaling which is also confirmed by our solution of the Stokes equation given in the previous section (cf. Appendix B).

Thus, the scaling of the Helmholz-Smoluchowski relation (Eq. 82) indeed holds with $\zeta = \zeta^{(0)} = -Q^{(0)}(z = 0^+) = \sigma$. The only difference is the dropped factor of $1/4$, which results from the decay of the tangential electric field within the diffuse layer, in contrast to the Helmholtz-Smoluchowski assumption of a uniform field applied in the bulk electrolyte. Note also that the first-order perturbed field due to membrane displacement acts on the leading-order base-state diffuse charge to drive electro-osmotic flow. This thus differs from other examples of ICEO flow [29], where the field acts on the perturbed charge, as discussed below. Taking into account the constant low-voltage capacitance of the diffuse layer $C_D^* = \epsilon\kappa$, the induced zeta potential is related to the total diffuse charge by $\zeta^* = \sigma^*/C_D^*$ [28,49]. In dimensionless units, we recover again $\zeta^{(0)} \simeq \sigma$. Using the incompressibility condition (58), we obtain the scaling $v_z(\mathbf{k}_\perp, z \to 0^+) \simeq k_\perp^2 h(\mathbf{k}_\perp)\sigma^2$. As illustrated in Fig. 4(b), the normal velocity is smaller than the tangential velocity by a factor $k_\perp$. Applying the boundary conditions $v_z(\mathbf{k}_\perp, z \to 0^+) = \partial h/\partial t$ together with equations (79-77), we find that the velocity estimated from this ICEO argument indeed corresponds to $\Gamma \simeq \sigma^2$ in the effective free energy of the membrane. Note that the velocity $v_z(\mathbf{k}_\perp, z \to 0^+)$ scales with the square of the applied electric field, so ICEO is relevant for both DC and AC electric fields, as long as the AC period exceeds the charging time (see below).

An equilibrium term in $k_\perp^3$, originating in unscreened dipole-dipole interactions, is also obtained in the calculation of Ref. [39], but in the high $k_\perp$ limit, in which $k_\perp L \gg 1$. It is absent in the low $k_\perp$ limit. Since the term we derive is obtained after taking $L \to \infty$, it is clear that the origin of this term is very different in both calculations and has an explicitly non-equilibrium origin in our approach.

In the remainder of this section, we give simple scaling arguments (with dimensions, for clarity) to highlight the basic physics of this new phenomenon of ICEO that we predict around driven membranes. For comparison, we first review the canonical example of ICEO flow around an ideally polarizable, uncharged metal post in a suddenly applied DC field E^* [29], illustrated in Fig. 5(a-c). We scale the geometry of the metal post to that of our curved membrane with an extent h^* parallel to the field and $k_\perp^{*-1}$ perpendicular to the field. In the base state (a) at $t = 0$, the metal post is an equipotential surface, but this is not a stable situation, since the surface is assumed not to pass any current. Instead, the normal current entering the diffuse layer charges it locally like a capacitor, until all the field lines are expelled (after the "RC" charging time $\tau_c^* \sim (D\kappa k_\perp^*)^{-1}$, where D is a characteristic ionic diffusivity [49]).
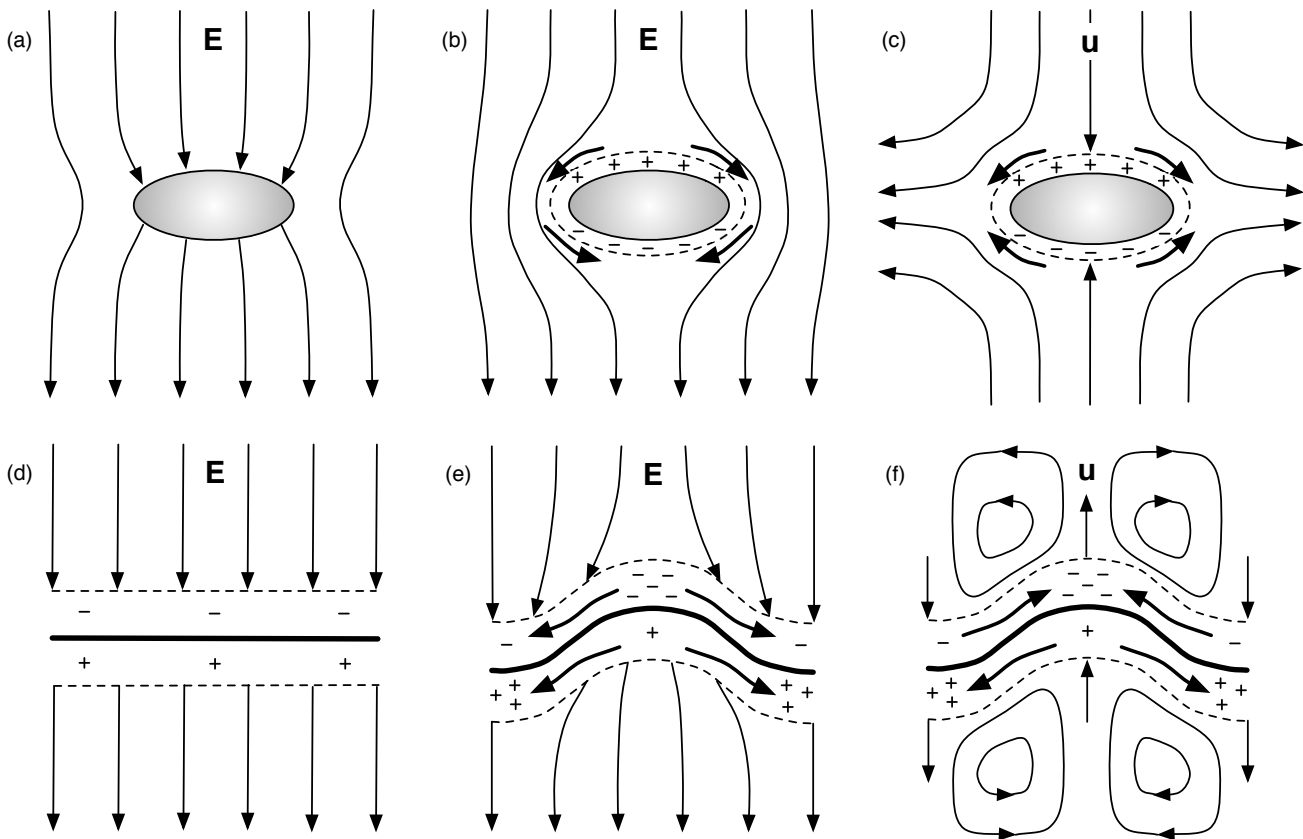
Fig. 5. The basic physics of ICEO around an ideally polarizable metal post [29] in (a-c), contrasted with our new example a driven membrane in (d-f). (a) The metal post is subjected to an electric field; (b) capacitive charging of the double layers screens the post and thus creates a tangential field (thick arrows); (c) the field acts on the induced diffuse charge to produce electro-osmotic slip (thick arrows) directed from the peak to the sides. (d) The membrane is subjected to an electric field, which drives a current through it, and creates small diffuse charge of the opposite sign (in the case of the first model of this paper, for which the membrane has a zero thickness); (e) the membrane shape fluctuates, inducing a shift in the diffuse charge and a tangential field (thick arrows); (f) the induced field acts on the initial charge to drive ICEO flow (thick arrows) in the reverse direction, from the valleys to the peaks.

The induced voltage across the diffuse layer scales as the background voltage applied across the post, $\zeta^* \sim E^* h^*$. The induced tangential electric field wraps around the post as shown in (b) and scales as $\mathbf{E}_\perp{}^* \sim E^* h^* \mathbf{k}_\perp^*$. Substituting into the slip formula (81) then yields the scaling of the ICEO velocity

$$\mathbf{v}_{\perp \, metal}^* \sim \frac{\epsilon \mathbf{k}_\perp^* h^{*2}}{\eta^*} E^{*2}, \qquad (87)$$

which flows in along the field axis toward the peak of the post and outward along its surface, as shown in (c).

In our model membrane, the ICEO flow is different in several important ways, although it shares the same basic principle of an applied field acting on its own induced diffuse charge around a polarizable surface. The physical picture is sketched in Figure 5(d-f). In this paper, we ignore diffuse-charge dynamics and focus on the steady response to shape perturbations. Initially, a normal field $E^* = E_z^{(0)*}$ is applied to the flat membrane to pass a current through it, as shown in (d). This induces a zeta potential scaling as

$\zeta^{(0)*} \sim -E^* \kappa^{-1}$ of opposite sign to the ideally polarizable metal post, due to the much lower "inner" capacitance of the membrane compared to the "outer" capacitance diffuse layers ($\delta_m \gg 1$), as explained above.

Now consider a fluctuation in the shape of the membrane, as shown in (e). Since $\delta_m \gg 1$, the membrane carries most of the voltage applied to the total double layer, so the perturbation of the induced zeta potential scales as $\zeta^{(1)*} \sim -E^* h^*$ since there is a transfer of this voltage (or the corresponding diffuse charge $q^{(1)*} \sim -\epsilon \kappa \zeta^{(1)*} = \epsilon E^* \kappa h^*$) from the diffuse layer on the protruding side to that of the other side.

As shown in (e), the induced tangential field, scaling as $\mathbf{E}_\perp^{(1)*} \sim \zeta^{(1)*} \mathbf{k}_\perp^*$, is the same on both sides of the membrane (even in z) and directed from the peaks ($h > 0$) to the valleys ($h < 0$) of the shape fluctuation. It may seem surprising that the field is bent away from the extra negative induced charge in the diffuse layer near the peak and toward the extra positive induced charge in the diffuse layer in the valley, but this is due to the large bound

positive (negative) charge on the upper (lower) side of the membrane, which greatly exceeds the diffuse charge in the regime $\delta_m \gg 1$). Ignoring the small diffuse charge, it becomes clear that the field is mainly perturbed to avoid the protrusion of the positively charged membrane.

Substituting these estimates in (81), we obtain the basic scaling of the ICEO velocity

$$\mathbf{v}_{\perp \, membrane}^{*} \sim -\frac{\epsilon \mathbf{k}_{\perp}^{*} h^{*}}{\eta^{*} \kappa} E^{*2} = -\frac{\mathbf{v}_{\perp \, metal}^{*}}{\kappa h^{*}} \qquad (88)$$

As in the example of the metal post, the ICEO flow around the membrane increases with the aspect ratio of the shape perturbation, $k_{\perp}^{*} h^{*}$, since it is associated with protrusions in the field direction. Compared to the ideally polarizable metal post (c), however, the curved membrane (f) exhibits "reverse" ICEO flow, which is directed from the valleys to the peaks. It is also reduced by a factor κh^{*}, which shows that ICEO flow around a driven membrane is inherently a phenomenon of thick double layers (compared to the shape perturbation amplitude). Although these flows are weak compared to large-scale ICEO flows in microfluidics and colloids in similar geometries, we have seen that they are strong enough to make a significant contribution to the small-scale dynamics of fluctuating biological membranes.

The physical mechanism sketched in Fig. 5(d-f) can be seen more clearly in Fig. 6, where the electric field and ICEO flow are shown for a shape perturbation of higher curvature with $k_{\perp}^{*} = h^{*} = \kappa$, where the double-layer thickness is comparable to the perturbation wavelength. In this regime, ICEO flow can no longer be understood purely as an effective slip given by (81), since normal forces on the fluid in Eq. (65) also play an important role in the flow. As described above, normal forces contribute to membrane motion and thus viscous flow of the type in Fig. 4(a), but they also produce osmotic pressure, which can drive flow relative to the instantaneous membrane position. For a thin quasi-equilibrium double layer, tangential gradients in osmotic pressure are balanced by electrical forces within the double layer and do not contribute to effective slip, as long as the bulk salt concentration is uniform [29,43,27]. For thick double layers, however, normal forces can also contribute to the flow, mainly within a distance of κ^{-1} from the peaks and valleys, and the associated flows have same scaling as Eq. (88).

A detailed study of how ICEO around a driven membrane depends on all the dimensionless parameters in our model would be interesting, but here we have focused on the regime $k_{\perp} \ll 1$, $\delta_m \gg 1$, $d \ll 1$ and $\delta_m \gg 1$. This regime corresponds to the first model discussed in this paper of a membrane of zero thickness and zero dielectric constant. As discussed in section 2, the sign of the charge distribution also depends on how conductive the membrane is as compared to the electrolyte. In real biological membranes the conditions $\delta_m \gg 1$ and $\delta_m \ll 1/G$ both hold simultaneously. In that case, due to the latter condition $\delta_m \ll 1/G$, the sign of zeroth order charge distribution is reversed as compared to that obtained in the first model of the paper, as shown in Fig. 2 and Fig. 5d. To summarize, to adapt these figures to the more biologically
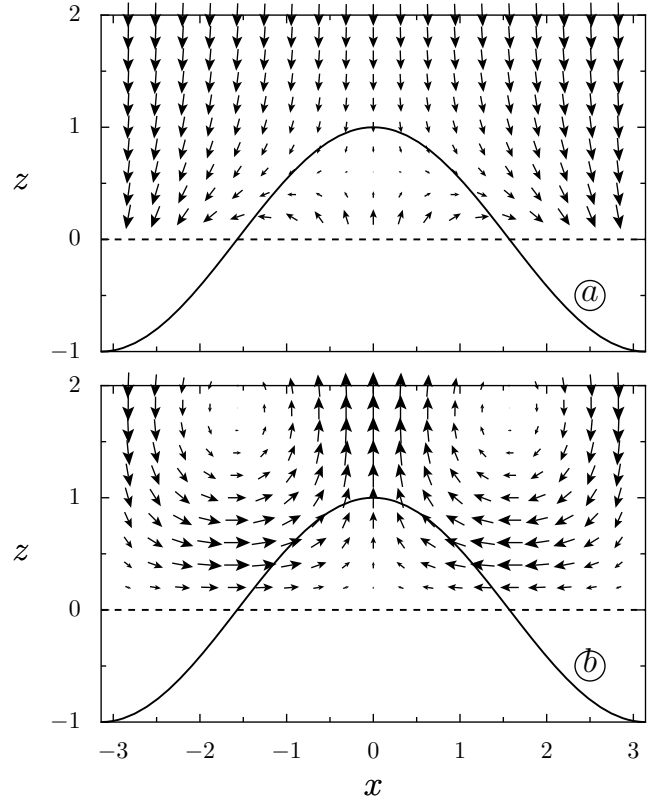

Fig. 6. Induced-charge electro-osmotic (ICEO) flow around a driven membrane in the regime of thick double layers $k_{\perp} = k_{\perp}^{*}/\kappa^{*} \approx 1$, where the thickness of the Debye layer is comparable to the wavelength of the shape perturbation and to the amplitude of modulation of the membrane. Indeed in units of the Debye layer, the amplitude of modulation of the membrane is 1, the wavevector is also 1 and the applied field corresponds to $\sigma = 8$. (a) The total electric field $\mathbf{E}$ avoids the protrusion peak due to the large positive bound charge on the membrane, even though the (much smaller) induced charge in the diffuse layer is negative at the peak and positive in the valley. (b) Vortices of induced-charge electro-osmotic flow, scaling as E^2, and driven from the valleys to the peaks by tangential fluid forces as in the thin double layer case of Fig. 4, but with stronger effects of normal forces in the recirculating regions, as explained in the text.

relevant case, one should reverse the sign of the charge distribution and that of the first order correction to the potential. Fortunately, since the ICEO flow velocity scales as the square of the electric field, the direction of the fluid flow shown in Fig. 5f will always be correct irrespective of the sign of the diffuse charge distribution.

4 Effects due to inhomogeneities in the pumps/channels concentration

We now discuss the effect of including the spatial dependance of the concentration field of the channels or pumps. The membrane free energy is modified by this concentra-

tion field. It is now written as

$$F_{mb} = \frac{1}{2} \int d^2\mathbf{r}_\perp [\kappa_0 \left(\nabla^2 h \right)^2 + \sigma_0 \left(\nabla h \right)^2 - 2\Lambda\phi\nabla^2 h + \beta\phi^2].$$ (89)

The new parameters Λ and β are the curvature-coupling coefficient and the compressibility associated with the channel concentration field respectively. Note that ϕ represents the deviation of the concentration field with respect to the uniform concentration. For simplicity, terms such as $(\nabla\phi)^2$, describing the energy cost of a non-uniform concentration field, have been ignored.

The equation of motion for the ϕ field follows from the above form of the membrane free energy. Gradients of chemical potential defined as $\mu_{mb} = \partial F_{mb}/\partial\phi$ provide the driving force for the motion of the channels on the membrane. Thus [38],

$$\frac{\partial\phi(\mathbf{k}_\perp)}{\partial t} = -k_\perp^2 [\Lambda k_\perp^2 h(\mathbf{k}_\perp) + \beta\phi(\mathbf{k}_\perp)].$$ (90)

In a linear approximation, the electrostatic potential can be written as a superposition of a base state contribution $\psi^{(0,0)}$, a contribution linear in the membrane height field $\psi^{(1,0)}$ and a contribution linear in the channel concentration field $\psi^{(0,1)}$. Augmenting our previous notation, $q^{(0,0)} = Q$, $c_k^{(0,0)} = N_k$ and $\psi^{(0,0)} = \Psi$ in the base state, we now have, instead of equation (44)

$$\begin{aligned} \psi(\mathbf{k}_\perp, z) &= \Psi(z) + \psi^{(0,1)}(\mathbf{k}_\perp, z) + \psi^{(1,0)}(\mathbf{k}_\perp, z), \\ q(\mathbf{k}_\perp, z) &= Q(z) + q^{(0,1)}(\mathbf{k}_\perp, z) + q^{(1,0)}(\mathbf{k}_\perp, z), \\ c_1(\mathbf{k}_\perp, z) &= N_1(z) + c_1^{(0,1)}(\mathbf{k}_\perp, z) + c_1^{(1,0)}(\mathbf{k}_\perp, z), \\ c_2(\mathbf{k}_\perp, z) &= N_2(z) + c_2^{(0,1)}(\mathbf{k}_\perp, z) + c_2^{(1,0)}(\mathbf{k}_\perp, z). \end{aligned}$$ (91)

The equations obeyed by $\psi^{(1,0)}$ and $q^{(1,0)}$, as well as $\psi^{(0,1)}$ and $q^{(0,1)}$ follow from equation (48).

For the contribution linear in the concentration field $\psi^{(0,1)}$ of the channels, the boundary conditions at the membrane surface impose continuity of the ion fluxes in the channels. Using the linear form for the conductances, we have

$$J_k = G_k\Delta\mu_k = \left(G_k^{(0,0)} + G_k^{(0,1)}\phi \right) \left(\Delta\mu_k^{(0,0)} + \Delta\mu_k^{(0,1)}\phi \right).$$ (92)

Collecting terms linear in ϕ, we obtain

$$J_k^{(0,1)} = \alpha_k^{(0,1)}\phi$$ (93)

with

$$\alpha_k^{(0,1)} = G_k^{(0,1)}\Delta\mu_k^{(0,0)} + G_k^{(0,0)}\Delta\mu_k^{(0,1)}.$$ (94)

We assume $\alpha_k = \alpha$, which represents the pumping rate. This condition only needs to be enforced at the unperturbed interface and along the z direction so that

$$\left(\partial_z q^{(0,1)} + \partial_z \psi^{(0,1)} \right)_{z=0} = \alpha\phi(\mathbf{r}_\perp).$$ (95)

We find the following solution for the electrostatic potential with these boundary conditions: for $z > 0$,

$$\psi^{(0,1)}(\mathbf{k}_\perp, z) = -q^{(0,1)}(\mathbf{k}_\perp, z) = \alpha\phi(\mathbf{k}_\perp) \left(\frac{e^{-lz}}{l} - \frac{e^{-k_\perp z}}{k_\perp} \right),$$ (96)

and for $z < 0$,

$$\psi^{(0,1)}(\mathbf{k}_\perp, z) = -q^{(0,1)}(\mathbf{k}_\perp, z) = \alpha\phi(\mathbf{k}_\perp) \left(\frac{-e^{lz}}{l} + \frac{e^{k_\perp z}}{k_\perp} \right).$$ (97)

Note that the corrections to the charge distribution and potential are odd functions of z in this case. This can be understood from the fact that the ion channels locally create a depletion of ions on one side and an increase of ion concentration on the other side. This depletion can be quantified through the jump in concentration of the charges across the membrane

$$q^{(0,1)}(\mathbf{k}_\perp, 0^+) - q^{(0,1)}(\mathbf{k}_\perp, 0^-) = -\frac{2\alpha\phi(\mathbf{k}_\perp)}{l}.$$ (98)

This jump in concentration provides an osmotic pressure difference between the two sides of the membrane, whose effect is irrelevant, however, since we have assumed the absence of permeation in writing the boundary condition of equation (68) [20].

The concentration field ϕ enters the equation of motion of the height field only through the membrane restoring force $\partial F_{mb}/\partial h$. This is because terms proportional to ϕ cancel in the difference of the stress along the z direction between both sides of the membrane in equation (69), due to the fact that $\psi^{(0,1)}(\mathbf{k}_\perp, z)$ is an odd function of z. As a consequence of this simplification, the transport coefficient α introduced in equation (95) does not enter the equation of motion for ϕ or for h. With equation (90), and the equation of motion for h,

$$\frac{\partial h(\mathbf{k}_\perp)}{\partial t} = -\frac{1}{4k_\perp}[((\sigma_0 + \Sigma)h(\mathbf{k}_\perp) + \Lambda\phi(\mathbf{k}_\perp)) k_\perp^2$$ (99)
$$+ h(\mathbf{k}_\perp)(\kappa_0 + K) k_\perp^4 + h(\mathbf{k}_\perp)\Gamma k_\perp^3],$$ (100)

the condition of stability of the membrane with its inclusions may be obtained, provided the bare elastic moduli of the membrane, and the induced surface charge σ, are known.

5 Electrically driven membrane of finite thickness

In this section, we consider a bilayer of finite thickness d and dielectric constant $\epsilon_m < \epsilon$. There is then an electrical coupling between the membrane and the surrounding electrolyte, with a strength measured by the parameter $t = \epsilon_m/(\kappa d^*\epsilon) = \delta_m^{-1}$ [12,7]. For equilibrium membranes, the importance of this coupling is discussed in refs. [15,9]. In dimensionless units, this coupling becomes r/d, where $r = \epsilon_m/\epsilon$ and d is the dimensionless membrane thickness.

For non-equilibrium driven membranes, capacitive effects associated with the finite thickness of the membrane dominate electrostatic corrections to the membrane elastic moduli, except at low ionic strength [26]. Further, capacitive effects are essential to explain voltage induced motion in cell membranes containing ion channels [10] and shape transitions of giant vesicles in AC electric fields [2].

We ignore variations in the concentration of the channels here [26]. We will also only consider the mode of fluctuation of the membrane in which each layer of the membrane fluctuates in phase with respect to each other, so that the position of each layer is $\pm d/2 + h(\mathbf{r}_\perp)$.

For simplicity, we only discuss the case of symmetric electrolytes: $n^- = n^+$, $D_1 = D_2 = D$, and $G_1 = G_2 = G$. We denote by ψ_m the internal potential for $|z| < d/2$ and ψ the electrolyte potential for $|z| > d/2$. When $t \neq 0$, the boundary conditions at the membrane are modified, becoming

$$\partial_z \psi^{(0)}(z \to \pm d/2) = r\partial_z \psi_m^{(0)}(z \to \pm d/2),$$
$$\psi^{(0)}(z \to \pm d/2) = \psi_m^{(0)}(z \to \pm d/2). \qquad (101)$$

The first equation is the continuity condition for the normal electric displacement and the second equation is the continuity condition of the potential.

We solve the analog of equations (5-6) together with an additional equation describing the region in between the bilayer. In this intermediate region, it is assumed that there is no charge density.

We find the following solution for the base state

$$E_z^{(0)}(z) = -\sigma - \tilde{\sigma} \exp\left(z + d/2\right), \text{ for } z < -d/2$$
$$E_z^{(0)}(z) = -\sigma - \tilde{\sigma} \exp\left(-z + d/2\right), \text{ for } z > d/2 \qquad (102)$$
$$E_m^{(0)} = -\frac{\sigma + \tilde{\sigma}}{r}, \text{ for } -d/2 < z < d/2.$$

Here σ still represents the surface charge of the Debye layers which is defined as in the case of zero thickness in equation (21). The current versus voltage relation obtained for zero thickness in equation (29) still holds in the finite thickness case, once L is replaced by $L - d$. Similarly equation (31) holds after replacing L^* by $L^* - d^*$, while equation (33) holds unchanged. In equation (102), we have introduced a new quantity $\tilde{\sigma}$ with the following property

$$\tilde{\sigma} = \int_{d/2}^{\infty} Q^+(z)dz = -\int_{-\infty}^{-d/2} Q^-(z)dz. \qquad (103)$$

Note that σ and $\tilde{\sigma}$ are related to each other by

$$\tilde{\sigma} = \frac{r\left(\sigma d - \sigma L + V\right) - \sigma d}{2r + d}. \qquad (104)$$

When dimensions are reinstated, one can see that only the diffusion time of the ions within a Debye layer enters in σ^* whereas $\tilde{\sigma}^*$ also contains the RC characteristic time of the membrane [26].

The boundary conditions for the first order correction in the membrane height field to the electrostatic potential and to the charge density are

$$\partial_z \psi^{(1)}(\mathbf{k}_\perp, \pm d/2) = \mp h(\mathbf{k}_\perp)\partial_z^2 \psi^{(0)}(d/2)$$
$$+ r\partial_z \psi_m^{(1)}(\mathbf{k}_\perp, \pm d/2), \qquad (105)$$

$$\psi^{(1)}(\mathbf{k}_\perp, \pm d/2) = \psi_m^{(1)}(\mathbf{k}_\perp, \pm d/2)$$
$$+ h(\mathbf{k}_\perp)\left(\partial_z \psi_m^{(0)} - \partial_z \psi^{(0)}\right)(d/2), (106)$$

$$\psi^{(1)}(\mathbf{k}_\perp, \pm\infty) = q^{(1)}(\mathbf{k}_\perp, \pm\infty) = 0, \qquad (107)$$

$$\partial_z q^{(1)}(\mathbf{k}_\perp, \pm d/2) + \partial_z \psi^{(1)}(\mathbf{k}_\perp, \pm d/2) = 0. \qquad (108)$$

The last equation corresponds to the boundary condition of zero flux in the first order solution. This condition was used in equation (51). The equations to first order in the height in the electrolyte regions $|z| > d/2$ are

$$\left(\partial_z^2 - k_\perp^2\right)\psi^{(1)}(\mathbf{k}_\perp, z) + q^{(1)}(\mathbf{k}_\perp, z) = 0, \quad (109)$$

$$\left(\partial_z^2 - k_\perp^2\right)\left(q^{(1)}(\mathbf{k}_\perp, z) + \psi^{(1)}(\mathbf{k}_\perp, z)\right) = 0, \quad (110)$$

subject to the boundary conditions given above.

The equations in the inside medium for $z < |d/2|$ are $q^{(1)}(\mathbf{k}_\perp, z) = 0$ and

$$\left(\partial_z^2 - k_\perp^2\right)\psi_m^{(1)}(\mathbf{k}_\perp, z) = 0. \qquad (111)$$

For $z > d/2$ and $z < -d/2$, $q^{(1)}(\mathbf{k}_\perp, z)$ and $\psi^{(1)}(\mathbf{k}_\perp, z)$ remain of the form $A\exp\left(\mp z + d/2\right)$, where A is a complicated function of $k_\perp, r, d, \sigma$ and $\tilde{\sigma}$. The first order correction to the potential in the inside medium has the form

$$\psi_m^{(1)}(\mathbf{k}_\perp, z) = \psi_m^{(1)}(\mathbf{k}_\perp, d/2)\frac{e^{k_\perp d/2}\left(e^{k_\perp z} + e^{-k_\perp z}\right)}{e^{k_\perp d} + 1}. \qquad (112)$$

In Figure 7, the potential $\Psi(z)$ and the quantity $Q(z)$ (which represents half the charge distribution) are shown in dimensionless units for two choices of parameters. These parameters correspond to a positive and a negative value of $\tilde{\sigma}$. The potential profiles illustrated in Figure 7 show that the sign of the electric field at the membrane surface ($\sim -\nabla\psi$) is controlled by the sign of $\tilde{\sigma}$. As shown in the appendix, in this case of a symmetric electrolyte and with the approximation $G_1 = G_2 = G$ the sign of $\tilde{\sigma}$ is positive when $\delta_m < 1/G$ and negative otherwise. The condition $\delta_m < 1/G$ is equivalent to $\epsilon_m/\epsilon \gg G^*/G_0^*$, where G^* is the typical conductance of typical ion channels/pumps and G_0^* is the conductance of a layer of electrolyte of thickness d^*. For real biological membranes, the membrane is typically much less conductive than the surrounding medium and thus $\delta_m < 1/G$. So the charge distribution in this case should be as the dashed line of Figure 7b, which has we mentioned earlier, has the opposite sign as compared to the charge distribution shown in Fig. 2.

5.1 Electrostatic corrections to elastic moduli

The Stokes equations can be solved as before, although the computations are now more involved. With the potential at zeroth and first order computed above, we first construct $\mathbf{f}(\mathbf{k}_\perp, z)$ using equations (65). After Fourier transforming in z, we insert the result in equation (??-66). From the solution of the Stokes equations, the velocity is obtained everywhere in the domain $|z| > d/2$.

We now have two boundary conditions for the stress tensor $\tau_{zz}^{(1)}$ at $z = \pm d/2$. Solving for the velocity field and extrapolating this velocity to $z = 0$, an effective free
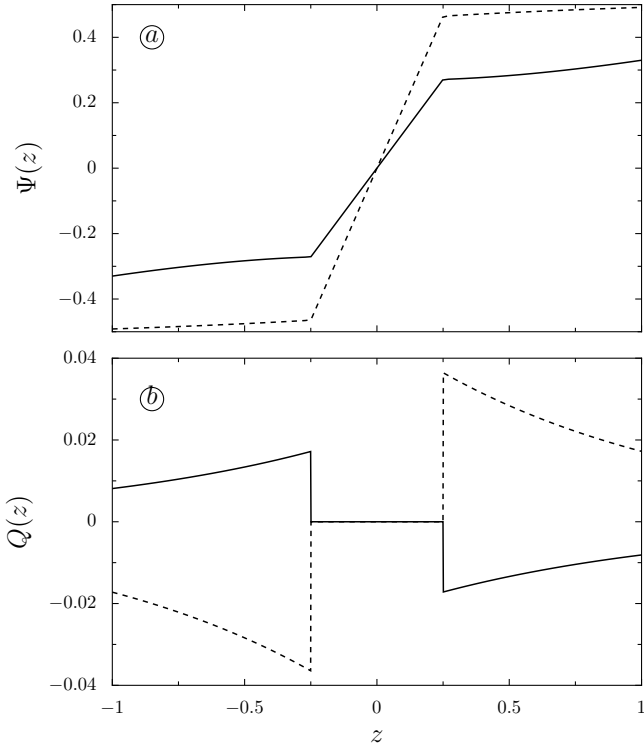
Fig. 7. Solutions of the electrokinetic equations for a membrane of finite thickness and symmetric ion concentrations. The electrostatic potential $\Psi(z)$ is shown in (a) and the quantity $Q(z)$ (which represents half the charge distribution) is shown in (b). We use dimensionless units and the following parameter values $L = 100$, $V = 2$, $G_1 = G_2 = 1$, $d = 0.5$, $r = 1/40$ and $k_\perp = 1$ for the solid line, and the same parameters except for $G_1 = G_2 = 0.01$ for the dashed line. For convenience, the potential represented in the solid line of (a) has been multiplied by an arbitrary factor of 10. For the solid line in (a), the curvature of the potential is positive near $z = d/2$, as in figure 2a, this corresponds to a negative value of $\tilde{\sigma}$. The charge distribution is as shown in the solid line of (b) and similar to figure 2b. For the dashed line in (a), the curvature of the potential is negative near $z = d/2$, this corresponds to a positive value of $\tilde{\sigma}$. Note that the sign of the charge distribution (dashed line in (b)) is reversed as compared to the solid line in (b).

energy of the same form as in equation (79) is obtained. The tension obtained from this calculation is the same as the one calculated from equation (42-43).

Both methods yield the result that the surface tension is the sum of an internal contribution Σ_{in}, arising from the contribution of the field lines which penetrate within the membrane, and an external contribution Σ_{out} associated to the field lines present in the Debye layers. These take the form[26]

$$\Sigma_{in} = -rdE_m^2 = -d\frac{(\sigma + \tilde{\sigma})^2}{r}, \qquad (113)$$

$$\Sigma_{out} = -\tilde{\sigma}^2 - 4\sigma\tilde{\sigma} + d\sigma^2, \qquad (114)$$

or

$$\Sigma_{in}^* = -\frac{(\sigma^* + \tilde{\sigma}^*)^2}{t\kappa\epsilon}, \qquad (115)$$

and

$$\Sigma_{out}^* = \frac{-(\tilde{\sigma}^*)^2 - 4\sigma^*\tilde{\sigma}^* + \kappa d^*(\sigma^*)^2}{\epsilon\kappa}, \qquad (116)$$

in terms of dimensionful quantities.

The negative contribution Σ_{in} is known as the Lippmann tension [10]. It is usually larger in absolute value than Σ_{out}. From equation (41), it follows that Σ_{in} is the electromagnetic energy of the internal field E_m contained within the space of the membrane. Since Σ_{in} is always negative, as illustrated qualitatively in Figure 3, the total membrane tension $\sigma_0 + \Sigma_{in} + \Sigma_{out}$ can become negative at some critical value of the internal field E_m, leading to the instabilities discussed in ref. [45]. Note that such an instability is present at zero wavelength, unlike the finite wavelength instability discussed from equation (75). Our calculations also yield the moduli

$$\Gamma = \frac{\sigma\tilde{\sigma}}{2}\left(8 + d^2 + 4d\right), \qquad (117)$$

and K, which is a complicated quadratic function of σ and $\tilde{\sigma}$.

All these moduli reach simple limiting values when the Debye length goes to zero ($\kappa \to \infty$ or equivalently $n^* \to \infty$). This limit is best understood in dimensionful notation. From equations (31-33), one finds that $i_k^* = -G_k^*V^*$ and $\sigma^* = 0$. From equation (104), we obtain $\tilde{\sigma} = rV/(2r + d)$. Using equation (32) we have

$$\tilde{\sigma}^* = \frac{k_BT\kappa\epsilon rV}{e(2r + d)} = \frac{\kappa\epsilon_m V^*}{2r + \kappa d^*}, \qquad (118)$$

which in the limit $\kappa \to \infty$ goes to $\epsilon_m V^*/d^*$.

The values of the moduli in this limit are independent of G, a consequence of the fact that electrical currents (i_k^* is non-zero) are not accompanied by charge accumulation in the Debye layers, because $\sigma^* = 0$. From equation (116), we find that $\Sigma_{out}^* = 0$. Using $t = r/\kappa d^*$ in equation (115), we find a non-zero limit for $\Sigma_{in}^* = -\epsilon_m(V^*)^2/d^*$. Thus the limit for the overall tension in the high salt limit is $\Sigma_0^* = -(V^*)^2\epsilon_m/d^*$. This resembles the energy of a plane capacitor with a voltage drop V^* and thickness d^*, although the system is not strictly analogous to a capacitor since electric currents are present (i_k^* is non-zero). For the bending modulus, the limiting value is

$$K_0^* = \frac{5(V^*)^2\epsilon_m d^*}{24}, \qquad (119)$$

and for Γ the limit is 0. The variation of Σ^*/Σ_0^* and of K^*/K_0^* as a function of the inverse Debye length κ are shown in Figure 4 for the case of zero and non-zero conductance.

Another limit of experimental relevance is that of small conductance $G \to 0$. In this limit, $\sigma = 0$ since there is no ion current in the medium as a consequence of i_k^* being zero. From equation (104), we obtain $\tilde{\sigma} = rV/(2r + d)$ which means $\tilde{\sigma}^* = V^*\epsilon\kappa t/(1 + 2t)$ in terms of dimensionful quantities. This shows that the membrane is a capacitor of surface charge $\tilde{\sigma}^* = -\epsilon_m E_m^* = V^*\epsilon\kappa t/(1 + 2t)$, where E_m^* is the internal field [26]. The equivalent circuit for this

problem is composed of three planar capacitors in series. One of these is the membrane (of capacitance per unit area ϵ_m/d) while the other two correspond to the Debye layers on each side (of capacitance $\epsilon\kappa$ per unit area), yielding a total capacitance $C^* = \epsilon\kappa t/(2t + 1)$.

Using equations (115-116), we find $\Sigma^*_{in} = -\tilde{\sigma}^2/t\kappa\epsilon$, $\Sigma^*_{out} = -\tilde{\sigma}^2/\kappa\epsilon$, and $\Gamma = 0$. The same expressions for the surface tension in the $G = 0$ limit were obtained recently using a different method in Ref. [39]. For comparison, we provide K^* for this case

$$K^* = \frac{1}{24r\epsilon\kappa^3}(\tilde{\sigma}^*)^2(18r + 5(\kappa d^*)^3$$
$$+ 24\kappa d^* r + 15(\kappa d^*)^2 r). \qquad (120)$$

Note that we recover the result of equation (119) when $\kappa \to \infty$.

This expression has some similarities as well as some differences with the expression for the bending modulus given in ref [39]. This discrepancy is likely to originate in the very different starting points for both calculations: the results of Ref. [39] are obtained from an explicitly equilibrium approach, whose results remain unchanged if hydrodynamic effects are incorporated. On the other hand, we begin with an explicitly non-equilibrium problem incorporating hydrodynamics from the outset.

It is unclear that it should simply suffice to set $G \to 0$ in our results to recover results derived for the equilibrium calculation. However, we note that in any case the predictions for K of both models are numerically very close and there is exact agreement for Σ. We also stress that both models predict that the electrostatic contribution to the bending modulus should increase with the salt concentration, whereas the electrostatic contribution to the surface tension should decrease with the salt concentration as illustrated in the solid lines of Figure 8. Both quantities also reach a well defined limit in the large salt concentration limit (see similar figure in ref [39]).

5.2 Numerical estimates, capacitive effects and fluctuation spectra

In the non-conductive limit (capacitor model), we find that $\Gamma = 0$. For $V^* = 50\text{mV}$, $L^* = 1\mu m$, $G = 0$, $D = 10^{-5}\text{cm}^2/s$, $n^* = 16.6\text{mM}$, $d^* = 5\text{nm}$ and $\epsilon_m/\epsilon = 1/40$, we have $\kappa^{-1} = 2.38\text{nm}$, $t = 1.2 \cdot 10^{-2}$, $\delta_m = 1/t = 84$ and $d = \kappa d^* = 2.1$, $V = eV^*/k_B T = 1.95$, $L = \kappa L^* = 419.7$. The elastic moduli are $\Sigma^*_{in} = -8.4 \cdot 10^{-6}$ Jm^{-2}, $\Sigma^*_{out} = -1.0 \cdot 10^{-7}$ Jm^{-2}, $\Gamma = 0$ and $K^* = 0.011 k_B T$. Let us now consider instead the case of a conductive membrane, with $G^* = 10\Omega^{-1}/\text{m}^2$, a value typical for ion channels [3]. This corresponds to a density of the potassium channels of 0.5 μm^{-2} and for $V^* = 50\text{mV}$, the electrical current going through the membrane is about 0.5A/m^2, which corresponds to about $3 \cdot 10^6$ ions going through a patch of $1\mu\text{m}^2$. The dimensionless channel conductance is $G = 3.8 \cdot 10^{-7}$. This very small value indicates that the membrane is significantly much less conductive than the electrolyte, and thus we are typically always in the regime

$\delta_m \ll 1/G$ for biological membranes. We also find that the order of magnitude of the tension and bending modulus are unchanged and a small value of $\Gamma^* = 8.2 \cdot 10^{-20}$ Jm^{-1} is found [26]. This indicates that the capacitor model with $G = 0$ is a good starting point for the calculation of the moduli in this case.

The importance of capacitive effects is confirmed by the observation that the values of the moduli obtained here are much larger than the corresponding estimates for the zero thickness case. This can be understood using an equivalent zero thickness model discussed in appendix A. Also, by varying the ionic strength in the case where ion transport is present ($G \neq 0$), we find that the capacitor model holds at high ionic strength but becomes invalid at low ionic strength, where ion transport has a stronger impact on the moduli.

This point is illustrated in Figure 8, where the electrostatic contribution to the tension Σ and the bending modulus K, as a function of the inverse Debye length κ in the $G = 0$ limit (solid line) and for $G^* = 10\Omega^{-1}/\text{m}^2$ (dashed line), are shown. The solid and dashed lines only deviate at small values of κ. The decrease of K/K_0 with salt concentration is also obtained in Ref. [40]. We have no simple explanation for the non-monotonicity of K/K_0 which is observed near $\kappa = 2 \cdot 10^6 \text{m}^{-1}$, but note that a qualitatively similar non-monotonicity - in the spontaneous curvature modulus, however - is seen in Ref. [40].

We find a reversal of the sign of Σ in the conductive case at small values of κ. The sign reversal is absent in the non-conductive case. This remarkable feature is shown in Figure 8(a). This mechanism of sign reversal may provide an explanation of some recent experiments, such as the study of cell movement of Ref. [10], where a reversal of movement/tension was observed in response to a change of ionic strength. This change of sign of the tension is clearly due to a change of sign of $\tilde{\sigma}$ as shown in Figure 3 (see also appendix for the condition of the change of sign of $\tilde{\sigma}$). One can see there that a change of sign of $\tilde{\sigma}$ occurs when the conductance G or the parameter δ_m are varied away from the point where $\tilde{\sigma} = 0$, which occurs when $\delta_m \simeq 1/G$.

Figures 9-10, show fluctuation spectra corresponding to the parameter values as indicated in the figure caption. The range of wavevectors indicated corresponds roughly to experimentally accessible values in video microscopy. Note the substantial increase of fluctuation amplitudes at low wavevectors in Figure 9, which arises from the lowering of the surface tension. Such a lowering is similar to the one observed in Ref. [46]. For the parameters used in Figure 10, corresponding to a larger bare tension σ_0^*, we see a significant increase of fluctuations over the full range of wavevectors.

6 Conclusion

In conclusion, we have analyzed the steady state fluctuations of a membrane driven by an applied DC electric field. Our analysis is valid in the linear regime for the response of the ion channels and for the description of the electrostatic
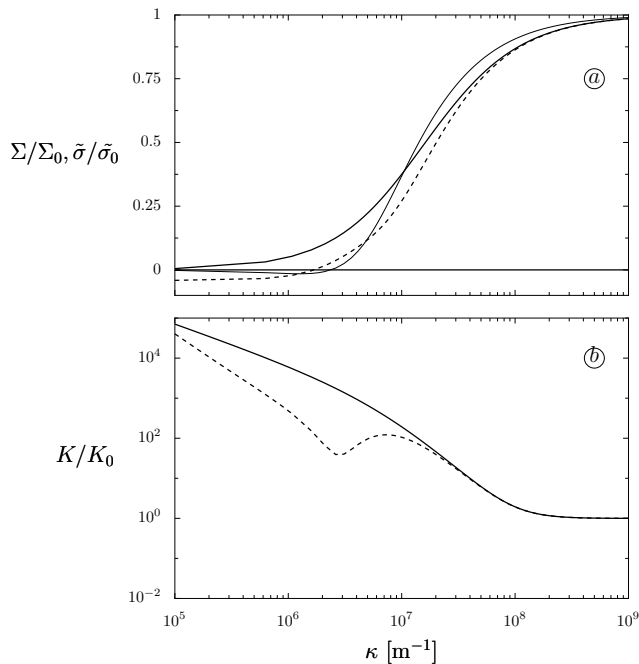
Fig. 8. Electrostatic contribution to the tension Σ and to the bending modulus K as a function of the inverse Debye length κ in the $G^* = 0$ limit (thick solid line) and for $G^* = 10\Omega^{-1}/\mathrm{m}^2$ (dashed line). (a) Ratios of normalized electrostatic contribution to the tension Σ/Σ_0 (dashed line for $G^* = 10\Omega^{-1}/\mathrm{m}^2$ and solid line for $G^* = 0$) and of $\tilde{\sigma}/\tilde{\sigma}_0$ (thin solid line for $G^* = 10\Omega^{-1}/\mathrm{m}^2$) are shown as function of κ. The tension Σ (resp. the surface charge $\tilde{\sigma}$) are normalized by their value in the infinite κ limit Σ_0 (resp. $\tilde{\sigma}_0$). Below $\kappa = 2 \cdot 10^6 \mathrm{m}^{-1}$, Σ/Σ_0 and $\tilde{\sigma}/\tilde{\sigma}_0$ both become negative when the membrane is conductive. No such change of sign is present in the tension in the non-conductive *i.e.* capacitor limit when $G = 0$ (thick solid line). For clarity the horizontal solid line represents the point of zero tension or zero of $\tilde{\sigma}$. (b) The ratio of normalized electrostatic contribution to the bending modulus K/K_0 is shown as a function of κ, where similarly K is normalized by its value in the infinite κ limit K_0. The $G^* = 0$ limit is represented as a thick solid line and the $G^* = 10\Omega^{-1}/\mathrm{m}^2$ case as a dashed line.

effects. We have confirmed the main results of Ref. [26], including the presence of a term proportional to $k_\perp^3$ in the fluctuation spectrum. We have provided a simple physical argument for the physics underlying this term, relating it to a nonlinear electrokinetic effect termed induced-charge electro-osmosis (ICEO). The predicted flow around a curved driven membrane is in the reverse direction from typical ICEO flows around blocking metal surfaces [29] and has different dependence on the geometry, in the limit we describe for the zero-thickness case. We stress, more generally, the importance of electrokinetic effects such as the one described here for descriptions of the dynamic properties of the soft, non-equilibrium membranes found in living cells.

Although our calculations addressed the case of a membrane driven out of equilibrium through the combined action of an external potential and ion channels or pumps which transferred ions across the surface, most of our re-
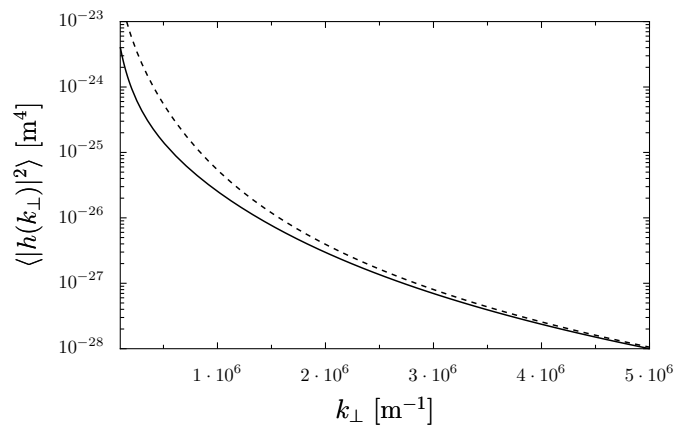

Fig. 9. Fluctuation spectrum of membrane fluctuations for the numerical values of the parameters discussed in the text. The solid line corresponds to the spectrum of a membrane of bare tension $\sigma_0^* = 10^{-7} \mathrm{Jm}^{-2}$ and bare bending modulus $\kappa_0^* = 15 k_B T$, while the dashed line corresponds to the fluctuation spectrum of a driven membrane in an electric field, which we describe with equation (80). The parameters are the same as discussed in the text except that here the potential drop which is applied is only of $V^* = 5\mathrm{mV}$, so that $\Sigma^* = -8.5 \cdot 10^{-8} \mathrm{Jm}^{-2}$, $\Gamma^* = 8.1 \cdot 10^{-22} \mathrm{Jm}^{-1}$ and $K^* = 0.0011 k_B T$.
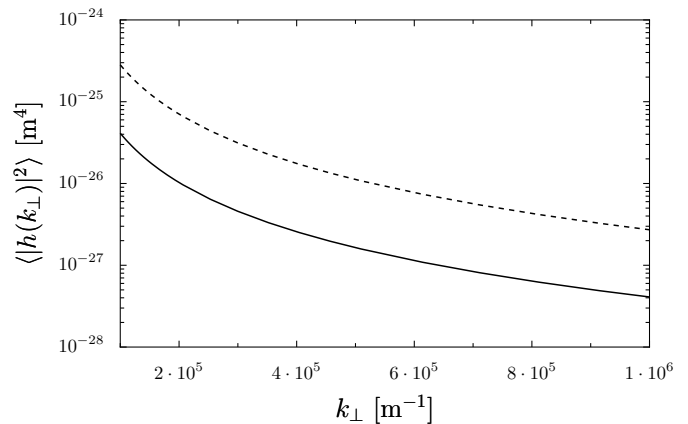

Fig. 10. Fluctuation spectrum of membrane fluctuations in the same conditions as in Figure 9 except for the potential $V^* = 50\mathrm{mV}$ and for the bare tension $\sigma_0^* = 10^{-5} \mathrm{Jm}^{-2}$.

sults should translate directly to the cell, where the potential difference across the membrane is maintained solely through active pumps and channels. This is a consequence of the observation that once steady currents are established which drive the system out of equilibrium, the precise way in which such transmembrane currents are maintained should be irrelevant to the description of membrane properties, which are dominated by effects at the much smaller scales of the bilayer thickness and the Debye screening length.

We have also confirmed the importance of capacitive effects, which are responsible for a negative contribution to the membrane tension and can lead to membrane insta-

bilities. In agreement with the recent results of Ref. [25], we find that the electrostatic and electrokinetic contribution to the bending modulus increases with the salt concentration, whereas the electrostatic contribution to the surface tension decreases with the salt concentration. We have also found a reversal of sign of the tension and of the surface charge in the Debye layer $\tilde{\sigma}$ in the low salt limit (as compared to the situation at high salt).

We have extended the calculations of Ref. [26] by including a channel concentration field in the description. This did not lead to qualitatively new effects within our perturbative treatment with our assumptions that the response of the channels to positive and negative ions is identical.

Extensions of the work described here include the description of non-equilibrium effects in membranes bearing a fixed charge which could be distributed asymmetrically across the two layers. The modulation of this fixed charge through remodeling of plasma membrane lipids is now understood to play an important role in cell division and phagocytosis. The cytoskeleton of the cell couples to the membrane, lending the coupled cytoskeleton-membrane system a shear modulus. In addition, cytoskeletal proteins are typically charged. Understanding how such effects modify the elastic properties of the coupled membrane-cytoskeleton system out of equilibrium is an area which is largely unexplored.

The clarification of the mechanical properties and fluctuation spectrum of lipid vesicles containing active pumps and channels is another possible application of the ideas presented here. Incorporating a biologically more reasonable model for the non-linear current voltage relation associated with ion pumps into the calculation would provide a useful extension of this work. Finally, achieving a more detailed understanding of the role of non-linear electrokinetic effects, such as ICEO, in modulating the dynamic properties of membranes driven out of equilibrium, appears to be an important new direction for further research.

A Mapping the finite membrane thickness model to zero thickness

The calculation of the electrostatic corrections in the case of a membrane of finite thickness is complex, leading to expressions which are often hard to interpret. It is thus useful to consider simpler, alternative formulations of the physics which could be used to gain physical insight. We

describe one such approach briefly below, based on the "Stern boundary condition" for thin dielectric layers [42], and use it to calculate the internal and external contributions to the surface tension.

The idea is to map the finite thickness problem into an equivalent zero-thickness one, but with boundary conditions which are different from the ones we considered in the body of the paper. Beginning with the definition

$$Q = \frac{1}{2}\left(\delta N_1 - \delta N_2\right), \tag{121}$$

following equations (8) we obtain

$$\partial_z^2 \Psi = -Q. \tag{122}$$

We can write the solutions to the problem for the $z > 0$ case as

$$\Psi(z) = \sigma\left(z - \frac{L}{2}\right) - Ae^{-z} + \frac{V}{2}, \tag{123}$$

and for the $z < 0$ case

$$\Psi(z) = \sigma\left(z + \frac{L}{2}\right) - A'e^z - \frac{V}{2}. \tag{124}$$

Applying the electrostatic boundary condition

$$r\partial_z \Psi_m(\pm\frac{d}{2}) = \partial_z \Psi(z = \pm\frac{d}{2}) \tag{125}$$

where the internal electric field is

$$E_m = -\partial_z \Psi_m(z). \tag{126}$$

The internal field is a constant which we can calculate from

$$\int_{-d/2}^{d/2} E_m(z)dz = dE_m = \Psi(-\frac{d}{2}) - \Psi(\frac{d}{2}). \tag{127}$$

This leads to the boundary condition

$$-\partial_z \Psi(z = \pm\frac{d}{2}) = \frac{r}{d}\left[\Psi(-\frac{d}{2}) - \Psi(\frac{d}{2})\right]. \tag{128}$$

We will now treat this as an equivalent zero thickness problem with the constraint that

$$\delta_m \partial_z \Psi(z = 0^\pm) = \Psi(0^+) - \Psi(0^-) \tag{129}$$

where

$$\delta_m = \frac{d}{r} = \frac{\epsilon d}{\epsilon_m} \tag{130}$$

is an effective length scale characterizing the membrane (scaled to κ^{-1}), over which the potential in the electrolyte extrapolates linearly to its value on the other side of the membrane. Note that equation (129) is a mixed Robin-type boundary condition, involving both the field Ψ and its derivative at the boundaries $z = 0^\pm$. In order to pass to the limit of zero membrane thickness, $d = d^*\kappa \to 0$, we take the joint limit $r = \epsilon_m/\epsilon \to 0$, keeping δ_m fixed. The boundary condition (129) also explicitly shows the

importance of the coupling parameter $t = \delta_m^{-1}$, which has been discussed for finite-thickness membranes [12,7,15,9].

The boundary condition equation (129) is now widely used to describe thin dielectric layers on metal surfaces and electrodes [49,42], although we are not aware of any prior application to ion-permeable membranes. It was perhaps first used to describe the compact Stern layer at the electrode/electrolyte interface [50] and recently extended to nonlinear surface capacitance [42]. In this context, it has been postulated that the field-dependent voltage drop, $\Delta\psi = \delta\,\partial_z\psi$, drives Faradaic electrochemical reactions [51, 42]. In our case, the same voltage drop contributes to electrochemical potential differences across the membrane, which set the ionic currents. In modeling ICEO flows around metal surfaces, the same boundary condition is also used to describe thin dielectric coatings, such as oxide layers [28,29,33], which is again similar to our modeling of ICEO flow around a driven membrane. The same type of Robin-type boundary condition has also been derived under more general conditions for the interface between a dielectric body (not necessarily a thin layer) and an electrolyte and used to model ICEO flows around dielectric microchannel corners and dielectric particles [36].

The physical interpretation of the parameter δ_m becomes more clear when written in terms of dimensional variables,

$$\delta_m = \frac{\epsilon\kappa}{\epsilon_m/d^*} = \frac{C_D}{C_m} \tag{131}$$

as the ratio of the low-voltage capacitance of the diffuse part of the double layer, $C_D = \epsilon\kappa$, to that of the compact part, $C_m = \epsilon_m/d^*$, which in our case is the membrane (but could also be a surface coating or Stern layer). In the linear regime of low voltages ($< kT/e$) and for thin double layers ($\kappa L \gg 1$, $d = d^*\kappa \gg 1$), these are constant capacitances, effectively in series [49], where $\delta_m(1+\delta_m)^{-1}$ is the fraction of the total double-layer voltage across the membrane, while $(1+\delta_m)^{-1}$ is the fraction across the diffuse layers.

There are two limiting cases of (129) which are commonly assumed in the literature [42]. In the "Gouy-Chapman limit" $\delta_m \ll 1$, most of the voltage drop occurs in the diffuse layer. In the "Helmholtz limit" $\delta_m \gg 1$, the compact layer – or in our case, the membrane – carries most of the voltage. We make the latter assumption in the main text to reduce equation (129) to the simpler boundary condition of equation (16).

Here, we briefly consider the general case $0 < \delta_m < \infty$. Using the above equations,

$$\partial_z\Psi(z=0^+) = \sigma + A,$$
$$\partial_z\Psi(z=0^-) = \sigma - A', \tag{132}$$

we have thus

$$\partial_z\Psi(z=0^+) = \partial_z\Psi(z=0^-) \implies A = -A' \tag{133}$$

We can fix A, using the result for $\Psi(z)$, yielding

$$A = \frac{V + \sigma(-\delta_m - L)}{2 + \delta_m}. \tag{134}$$

Comparing equations (132) with equation (102), we see that $A = \tilde{\sigma}$ and equation (134) are equivalent to equation (104) in the limit $r \to 0, d \to 0$, keeping δ_m fixed.

We now illustrate the calculation of the tension, using our earlier result

$$\Sigma^{out} = -\int_{-L/2}^{L/2} (E_z^{(0)})^2(z)dz$$
$$+ \frac{L}{2}\left[(E_z^{(0)})^2(z \to \infty) + (E_z^{(0)})^2(z \to -\infty)\right] \tag{135}$$

which yields

$$\Sigma^{out} = -2\int_0^{L/2} E^2(z)dz + LE^2(z \to \infty)$$
$$= -2\int_0^{L/2} (\sigma + Ae^{-z})^2 dz + L\sigma^2$$
$$= -2\int_0^{L/2} (\sigma^2 + A^2e^{-2z} + 2\sigma Ae^{-z})dz + L\sigma^2$$
$$= -2\left[\frac{A^2}{2} + 2\sigma A\right], \tag{136}$$

which goes to $3\sigma^2$ in the limit of $\delta_m \to 0$ for the zero thickness limit, where $A = -\sigma = \tilde{\sigma}$. We can also obtain

$$\Sigma^{in} = -rE_m^2 = \frac{-r}{d^2}\left[\Psi(0^+) - \Psi(0^-)\right]^2 = -\frac{d}{r}(\sigma + A)^2 \tag{137}$$

which coincides with equation (113) given in the main text.

Using the definition of σ of equation (21), and the expression of the ion fluxes of Eqs. (29)-(30), we have that $\sigma \simeq GV/(1 + GL)$. From equation (134), one obtains

$$A \simeq \frac{V}{(1 + GL)(2 + \delta_m)}(1 - G\delta_m), \tag{138}$$

which shows that $A > 0$ when $\delta_m < 1/G$ and $A < 0$ when $\delta_m > 1/G$. The condition $\delta_m < 1/G$ is equivalent to $\epsilon_m/\epsilon \gg G^*/G_0^*$, where G^* is the typical conductance of typical ion channels/pumps defined in equation (25) and $G_0^* = Dn^*e^2/d^*k_BT$ is the conductance of a layer of electrolyte of thickness d^*.

B Solution of the Stokes equations for the first model of a membrane of zero thickness and zero dielectric constant

We recall that the normal component of the velocity satisfies a single fourth order differential equation, Eq. 67. With the expressions for the charge and the potential at zeroth and first order given in the previous sections, the flow can be solved on each side separately as

$$v_z(\mathbf{k}_\perp, z) = (A_1 + B_1z)e^{-k_\perp z} + C_1e^{-lz} \quad \text{for } 0 < z\,,$$
$$v_z(\mathbf{k}_\perp, z) = (A_2 + B_2z)e^{k_\perp z} + C_2e^{lz} \quad \text{for } z < 0\,,$$

where the integration constants must be determined by proper matching boundary conditions. Note that the boundary conditions on the membrane are enforced at $z = 0^{\pm}$ rather than at the actual position $h(\mathbf{r})$ of the interface because of our assumption of small deformations limited to first order in the membrane height.

Imposing the boundary conditions for the velocity of Eqs. 68-71, the flow on the positive side $z > 0$ is explicitly calculated to be

$$v_z(\mathbf{k}_\perp, z) = \sigma^2 k_\perp^2 \left(z - \frac{1}{l} - \frac{zk_\perp}{l} \right) e^{-k_\perp z} h(\mathbf{k}_\perp) \quad (139)$$

$$+ \, s \left(1 + zk_\perp \right) e^{-k_\perp z} h(\mathbf{k}_\perp) \quad (140)$$

$$+ \, \frac{\sigma^2 k_\perp^2}{l} e^{-lz} h(\mathbf{k}_\perp), \quad (141)$$

and

$$\mathbf{v}_\perp(\mathbf{k}_\perp, z) = -i\mathbf{k}_\perp \sigma^2 \left(-1 + k_\perp z - \frac{k_\perp^2 z}{l} \right) \quad (142)$$

$$\times \, e^{-k_\perp z} h(\mathbf{k}_\perp) - zsi\mathbf{k}_\perp h(\mathbf{k}_\perp) e^{-k_\perp z} \quad (143)$$

$$- \, i\sigma^2 \mathbf{k}_\perp h(\mathbf{k}_\perp) e^{-lz}. \quad (144)$$

Note that, at this point, the stress boundary conditions have not been used yet. In the particular case where no electrostatic force is present (for $\sigma = 0$), one recovers the fluid flow created with a membrane bending mode [48], which is represented in Fig. 4a.

$$v_z(\mathbf{k}_\perp, z) = s \left(1 + zk_\perp \right) e^{-k_\perp z} h(\mathbf{k}_\perp), \quad (145)$$

$$\mathbf{v}_\perp(\mathbf{k}_\perp, z) = -i\mathbf{k}_\perp zs e^{-k_\perp z} h(\mathbf{k}_\perp). \quad (146)$$

In the general case where $\sigma \neq 0$, we are interested in the solution of the Stokes equation where the growth rate s is determined from the stress boundary conditions. For Fig. 4b and Figs. 6, we have assumed that $s = 0$, which corresponds to a quasi-stationary membrane, whose shape is determined by the flow field.

The stress component along z, obtained to first order in the membrane height field and evaluated at the membrane surface, is

$$\tau_{zz}^{(1)} = -p + 2\partial_z v_z + \partial_z \psi^{(1)} \partial_z \Psi + h(\mathbf{r}_\perp)\partial_z \left[-P + (\partial_z \Psi)^2/2 \right]. \quad (147)$$

As follows from equations (22,23), and (40), the stress is balanced in the base state. Thus, the last term drops out and

$$\tau_{zz}^{(1)} = \left(-p + 2\partial_z v_z + \partial_z \psi^{(1)} \partial_z \Psi \right)_{z=0}. \quad (148)$$

Similarly the transverse stress is

$$\tau_{\perp z}^{(1)} = \left(\partial_\perp v_z + \partial_\perp \psi^{(1)} \partial_z \Psi \right)_{z=0}. \quad (149)$$

In fact, because of our use of the boundary condition of a vanishing electric field on the membrane, these expressions further simplify to $\tau_{zz}^{(1)} = (-p + 2\partial_z v_z)_{z=0}$ and $\tau_{\perp z}^{(1)} = (\partial_\perp v_z)_{z=0}$. These stresses can be evaluated using

the expression of the pressure in terms of v_z and $\mathbf{f}_\perp$, while v_z itself can be obtained by solving Eq. 67.

With the expressions of the velocity given in Eqs. 139-142, the discontinuity in the normal-normal stress Eq. 73 component fixes the value of the growth rate s. After expanding the obtained expression in powers of $k_\perp$, one obtains the growth rate equation given in Eq. 77.

After inserting the expression of the growth rate s into the equations for the flow field given in Eqs. 139-142 and Taylor expanding with respect to $k_\perp$, one finds that (at lowest order in $k_\perp$)

$$\mathbf{v}_\perp(\mathbf{k}_\perp, z) \simeq i\mathbf{k}_\perp h(\mathbf{k}_\perp)\sigma^2 \left(1 - e^{-z} \right), \quad (150)$$

which is essentially the result of Eq. 86. This result confirms that the tangential velocity $\mathbf{v}_\perp$, which is strictly zero at $z = 0$ according to the non-slip boundary condition, has a significant (non-zero) value at a distance z of the order of one Debye length away from the interface, as predicted from the Helmholz-Smoluchowski formula of Eq. 81.

References

1. For an extensive review, see U. Seifert, Adv. Phys. **46**, 13 (1997).
2. R. Dimova, K. A. Riske, S. Aranda, N. Bezlyepkina, R. Knorr and R. Lipowsky, Soft Matter, **3**, 817 (2007).
3. B. Hille, *Ion Channels of Excitable Membranes*, (Sinauer Press, Sunderland MA, 2001).
4. E. Kandel, J. Schwartz and T. Jessel, *Principles of Neural Science*, (MacGraw-Hill, New York, 2000).
5. T. Yeung, M. Terebiznik, L. Yu, J. Silvius, W. M. Abidi, M. Philips, T. Levine, A. Kapus and S. Grinstein, Science **313**, 347 (2006).
6. S. Lecuyer, G. Fragneto and T. Charitat, Eur. Phys. J. E **21**, 153 (2006).
7. D. Andelman, in *Handbook of Biological Physics*, edited by R. Lipowsky and E. Sackmann, (Elsevier, Amsterdam, 1995).
8. P. Pincus, J.-F. Joanny and D. Andelman, Europhys. letters **11**, 763 (1990).
9. T. Chou, M. V. Jaric and E. Siggia, Biophysical Journal, **72**, 2042 (1997).
10. P-C. Zhang, A. M. Keleshian, and F. Sachs, Nature, **413**, 428 (2001).
11. B. Duplantier, R. E. Goldstein, V. Romero-Rochin, and A. I. Pesci, Phys. Rev. Lett., **65**, 508 (1990); R. E. Goldstein, A. I. Pesci, V. Romero-Rochin, Phys. Rev. A **41**, 5504 (1990).
12. M. Winterhalter and W. Helfrich, J. Phys. Chem., **92**, 6865 (1988); *ibid* **96**, 327 (1992).
13. H. N. W. Lekkerkerker, Physica A, **159**, 319 (1989).
14. S. T. Milner, J.-F. Joanny and P. Pincus, Europhys. Lett., **9**, 495 (1989).
15. M. Kiometzis and H. Kleinert, Phys. Lett. A, **140**, 520 (1989).
16. J. Prost and R. Bruinsma, Europhys. Lett., **33** (4), 321 (1996).
17. S. Ramaswamy, J. Toner, and J. Prost, Phys. Rev. Lett. **84**, 3494 (2000).

18. S. Ramaswamy and M. Rao, C. R. Acad. Sci. Paris. t. 2, Série IV, 817 (2001).

19. J.-B. Manneville, P. Bassereau, D. Lévy and J. Prost, Phys. Rev. Lett. **82**, 4356 (1999).

20. J.-B. Manneville, P. Bassereau, S. Ramaswamy, and J. Prost, Phys. Rev. E **64**, 021908 (2001).

21. S. Sankararaman, G. I. Menon, and P. B. S. Kumar, Phys. Rev. E, **66**, 031914 (2002)

22. D. Lacoste and A. W. C. Lau, Europhys. Lett. , **70** (3), 418 (2005).

23. H.-Y. Chen, Phys. Rev. Lett., **92** (16), 168101 (2004).

24. M. C. Sabra and O. G. Mouritsen, Biophys. J., **74**, 745 (1998).

25. M. A. Lomholt, Phys. Rev. E, **73**, 061913 (2006); Phys. Rev. E, **73**, 061914 (2006).

26. D. Lacoste, M. Cosentino Lagomarsino, and J. F. Joanny, Europhys. Lett., **77**, 18006 (2007).

27. W. B. Russel, D. Saville, and W. R. Schowalter, *Colloidal Dispersions* (Cambridge University Press, Cambridge, England, 1989); R. J. Hunter, *Foundations of Colloid Science* (Oxford University Press, 2001); .

28. A. Ajdari, Phys. Rev. E **61**, R45 (2000); A. González, A. Ramos, N. G. Green, A. Castellanos and H. Morgan, Phys. Rev. E, **61**, 4019 (2000).

29. M. Z. Bazant and T. M. Squires, Phys. Rev. Lett., **92** (6), 066101 (2004); T. M. Squires and M. Z. Bazant, J. Fluid Mech. **509**, 217-252 (2004); **560**, 65 (2006).

30. V. Kumaran, Phys. Rev. E, **64**, 011911 (2001); R. Thaokar and V. Kumaran, Phys. Rev. E, **66**, 051913 (2002); V. Kumaran, Phys. Rev. Lett., **85**, 4996 (2000).

31. V. A. Murtsovkin, Kolloidn. Zh. **58**, 358 (1996).

32. A. Ramos, H. Morgan, N. G. Green, and A. Castellanos, J. Colloid Interface Sci. **217**, 420 (1999); N. G. Green, A. Ramos, A. Gonzalez, H. Morgan, and A. Castellanos, Phys. Rev. E **61**, 4011 (2000).

33. J. A. Levitan, S. Devasenathipathy, V. Studer, Y. Ben, T. Thorsen, T. M. Squires, and M. Z. Bazant, Colloids and Surfaces A **267**, 122 (2005).

34. C. K. Harnett, J. Templeton, K. A. Dunphy-Guzman, Y. M. Senousy and M. P. Kanouff, Lab on a Chip, **8**, 565 (2008).

35. S. K. Thamida and H. C. Chang, Phys. Fluids **14**, 4315 (2002).

36. G. Yossifon, I. Frankel, and T. Miloh, Phys. Fluids **18**, 117108 (2006); **19**, 068105 (2007).

37. S. Gangwal, O. J. Cayre, M. Z. Bazant, and O. D. Velev, Phys. Rev. Lett. **100**, 058302 (2008).

38. F. Divet, G. Danker and C. Misbah, Phys. Rev. E, **72**, 041901 (2005).

39. T. Ambjörnsson, M. A. Lomholt, P. L. Hansen, Phys. Rev. E, **75**, 051916 (2007).

40. S. Chatkaew and M. Leonetti, Eur. Phys. J. E **17**, 203 (2005); M. Leonetti, E. Dubois-Violette, and F. Homblé, PNAS, **101**, 10243 (2004); M. Leonetti and E. Dubois-Violette, Phys. Rev. Lett., **81**, 1977 (1998).

41. J. D. Jackson, *Classical Electrodynamics*, 3rd edn, (Wiley, 1999).

42. M. Z. Bazant, K. T. Chu, and B. J. Bayly, SIAM J. Appl. Math. **65**, 1463 (2005); K. T. Chu and M. Z. Bazant, SIAM J. Appl. Math. **65**, 1485 (2005).

43. B. Zaltzman and I. Rubinstein, J. Fluid Mech. **579**, 173 (2007).

44. J. S. Rowlinson and B. Widom, *Molecular Theory of Capillarity* (Oxford University Press, Oxford, 1982).

45. P. Sens and H. Isambert, Phys. Rev. Lett., **88**, 128102 (2002).

46. M. D. El Alaoui Faris, D. Lacoste, J. Pécréaux, J-F. Joanny, J. Prost and P. Bassereau, http://arxiv.org/abs/0807.0081 (manuscript currently under review).

47. T. Bickel, Phys. Rev. E **75**, 041403 (2007).

48. A. Levine and F. C. MacKintosh, Phys. Rev. E, **66**, 061606 (2002).

49. M. Z. Bazant, K. Thornton, and A. Ajdari, Phys. Rev. E **70**, 021506 (2004)

50. E. M. Itskovich, A. A. Kornyshev, and M. A. Vorotyntsev, Phys. Status Solidi A **39**, 229 (1977).

51. A. Bonnefont, F. Argoul, and M. Z. Bazant, J. Electroanal. Chem. **500**, 52 (2001).